STU

Slovak University of Technology
Faculty of Electrical Engineering and Information Technology

Ondrej Pohorelec

Hole Channel GaN Based Transistor for Power Electronics

Dissertation thesis abstract

to obtain the Academic Title of philosophiae doctor abbreviated as "PhD."

in the doctorate study programme: Electronics and photonics
in the field of study: Electrical and Electronics Engineering
Form of study: full-time

Bratislava, June 2023

STU

Dissertation Thesis has been prepared at:

Institute of Electrical Engineering, Slovak Academy of Sciences

Submitter Ing. Ondrej Pohorelec
Institute of Electrical Engineering SAS
Dúbravská cesta 9
841 04 Bratislava

Supervisor RNDr. Dagmar Gregušová, DrSc.
Institute of Electrical Engineering
Slovak Academy of Sciences

Readers prof. Ing. Ivan Hotový, DrSc.
Faculty of Electrical Engineering and Information Technology
Slovak University of Technology

Ing. Karol Čičo, PhD.
Semikron Danfoss

Dissertation Thesis Abstract was sent: .....

Dissertation Thesis Defence will be held on .....

at ..... at .....

prof. Ing. Vladimír Kutiš, PhD.
(Dean of the Faculty)

Slovak University of Technology in Bratislava
Institute of Electronics and Phototonics

Faculty of Electrical Engineering and Information Technology
Academic year: 2022/2023
Reg. No.: FEI-104404-72651

DISSERTATION THESIS TOPIC

Student:	**Ing. Ondrej Pohorelec**
Student's ID:	72651
Study programme:	Electronics and Photonics
Study field:	Electrical and Electronics Engineering
Thesis supervisor:	RNDr. Dagmar Gregušová, DrSc.
Head of department:	doc. Ing. Anton Kuzma, PhD.
External educational institution:	Institute of Electrical Engineering of the Slovak Academy of Sciences

Topic: **Hole Channel GaN-based Transistor for Power Electronics**

Language of thesis: English

Specification of Assignment:

Analyze the reliability of E-mode transistors with unintentional hole channel

Prepare InAlN/GaN heterostructures with hole-type conductivity

Analyze the structural and electrical properties of the prepared structures

Based on the obtained results, assess the viability of the InAlN/GaN transistor with hole conductivity

Deadline for submission of Dissertation thesis:	31. 05. 2023
Approval of assignment of Dissertation thesis:	19. 06. 2023
Assignment of Dissertation thesis approved by:	prof. Ing. Viera Stopjaková, PhD. – Chairperson of the field of study board

STU

Contents

STU

Objectives of the dissertation thesis

- Analyze the reliability of E-mode transistors with unintentional hole channel
- Prepare InAlN/GaN heterostructures with hole-type conductivity
- Analyze the structural and electrical properties of the prepared structures
- Based on the obtained results, assess the viability of the InAlN/GaN transistor with hole conductivity

1 Introduction

With technological progress comes the need for more power and faster data transmission for all the electronic devices. Silicon - the most perfected and used semiconductor material for several decades - is reaching is physical limits in both power and high frequency applications.

GaN is one of the materials that could replace Si in various applications. GaN-based high electron mobility transistors (HEMTs) are already commercially available, there are even various consumer power adapters and chargers available in the market. Wide band gap semicondcutors, particularly GaN and SiC are making their way into the electric vehicles in the form of DC-DC converters [1]. In the RF applications, GaN can be used in the 5G networks [2].

While GaN devices are already available, there is still an intense research in various areas. GaN HEMTs are typically normally-on or depletion mode devices. It means that at zero voltage on the gate electrode transistor is conducting current between source and drain electrode. In case of a power or other failure of the control circuit this might be dangerous, so there is a considerable effort to develop normally-off transistors.

There are various approaches to achieve positive threshold voltage - polarization engineering, p-GaN gate or reduction of surface donors. Technological processes to prepare these devices are much more difficult and often introduce problems that cause reliability issues.

One part of the thesis deals with threshold voltage instabilities of normally-off device prepared with a polarization engineering approach. Positive threshold voltage was achieved by an addition of InGaN cap layer, which in turn creates an unintentional hole channel in the heterostructure. The additional two-dimensional hole channel (2DHG) is partly responsible for a threshold voltage shift in the opposite direction to what was observed for normally-on HEMTs.

There is also an effort to monolithically integrate control circuits with power circuits. To replicate CMOS-like logic circuits on GaN, transistors with both electron and hole channels are necessary. High performance transistors with 2DHG are still a challenge as they suffer from low mobilities and hole densities compared to the devices with 2DEG.

The second part of the thesis deals with the creation of the hole channel in the

InAlN/GaN heterostructure. Magnesium, a p-type dopant, was used to attempt to increase hole density in the channel.

Mg doping of In-rich InAlN layers was investigated further in the third part of the thesis, where InAlN was doped to increase the resistivity in order to use it as a buffer layer. However, the results might provide insight into Mg doping of other layers with different In content.

2 Theoretical background

2.1 III-N Semiconductor materials

III-N semiconductors are materials consisting of one or more elements from III-group element (Al, Ga, In) and nitrogen.

Due to large bandgap, high breakdown voltage, and high electron mobility, theses materials can be used in high power and high frequency electronics. III-nitrides are direct semiconductors and their bandgap can be adjusted from UV to IR, making them viable material for various optoelectronic applications. Other properties are depicted in Fig. 2.1 in comparison with other materials.

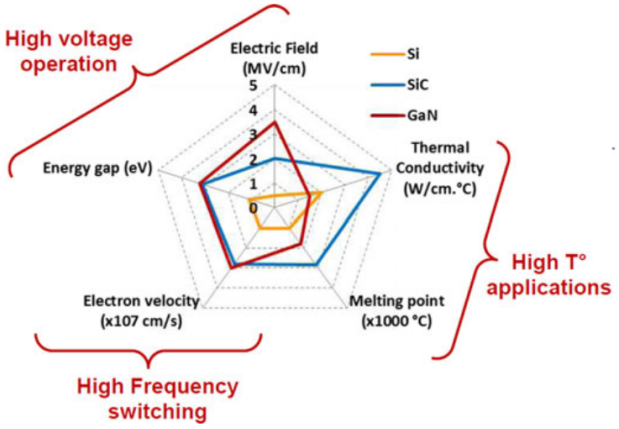

Figure 2.1: Summary of selected semiconductor properties of GaN, Si and SiC [3].

$In_xAl_{1-x}N$ is an interesting ternary alloy in the III-N group semiconductors. By changing In content, bandgap can be tuned from 0.7 eV for InN up to 6.02 eV for AlN. Moreover, InAlN can be lattice matched to GaN at x=0.17. In that case 2DEG is created solely due to spontaneous polarization, with fewer dislocation because of no strain [4]–[6]. InAlN as a barrier layer might also provide improvement over AlGaN/GaN HEMTs [7].

2.2 Polarization Effects

Wurtzite strucutre has polarization axis parallel to c-axis (0001). Due to slight deviations of the real crystal lattice from the ideal wurtzite lattice, there is a macroscopic spontaneous polarization present [8]. This polarization creates internal electric field.

If we grow different material on GaN, we introduce lattice strain to the heterotructure. This creates piezoelectric polarization, which can have either direction, depending on the strain whether it is compressive or tensile.

Gradient of the polarization at the interface induces a sheet charge density. Free charge carriers will compensate this polarization induced sheet charge density. If the sheet charge density is positive electrons will accumulate on the interface, creating 2DEG, if the sheet charge density is negative, holes will accumulate and create a 2DHG [9].

2.3 Threshold Voltage Instabilities

Positive Bias Temperature Instabilities (PBTI) and Negative Bias Temperature Instabilities (NBTI) are a reliability concern in modern semiconductor technologies. They can impact the functionality and lifetime of integrated circuits, leading to performance degradation, reduced operational speed, and potential device failure.

There are various causes of threshold voltage instabilities. Some of the most severe are caused by oxide traps or interface traps between oxide and semiconductor. Band diagrams of Al_2O_3/AlGaN/GaN heterostructure with oxide and interface traps are depicted in Fig. 2.2 [10].

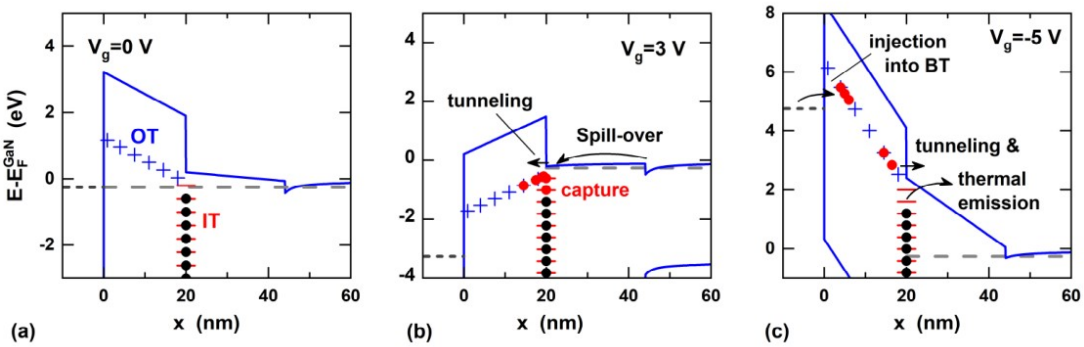

Figure 2.2: Band diagram of Al_2O_3/AlGaN/GaN heterostructure. (a) at $V_{GS} = 0V$ heterostructure is in thermal equilibrium, (b) at $V_{GS} = 3V$ empty traps above Fermi level are filled with electrons and (c) at $V_{GS} = -5V$ with various possible emission and capture processes [10].

Typical PBTI measurement is presented in Fig. 2.3. During the stress period, the threshold voltage experiences a positive drift as a result of electron trapping in

the interface and oxide traps. Subsequently, during the recovery phase, the threshold voltage undergoes a shift towards negative values as electrons are emitted from the traps. However, it should be noted that the threshold voltage does not completely return to its initial position (represented by the dashed line) due to the presence of traps with longer time constants compared to the measurement time.

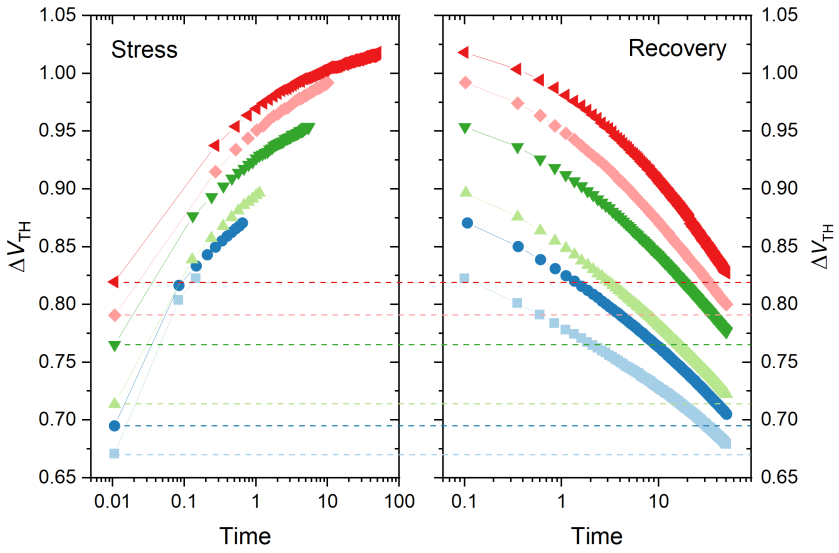

Figure 2.3: Threshold voltage drift measurement by the MSM method. Stress period is on the left and recovery period is on the right.

3 State of the art

3.1 Normally-off transistors

Normally-off transistors are needed for logic circuits [11] and safe operation of high-performance switches [12], because they default to off-state in case of a failure of the control circuit. There are several approaches to achieve higher positive voltage without sacrificing the quantum well channel. Some of them are p-GaN capping [13], fluoride implantation to barrier [14], [15], reduction of surface donor density [16] or polarization engineering [17], [18].

Polarization Engineering

Polarization engineering uses the polarization induced electric fields in III-nitrides to manipulate energy bands. One of the options is to use InGaN on top of AlGaN/GaN heterostructure [17] (Fig. 3.1).

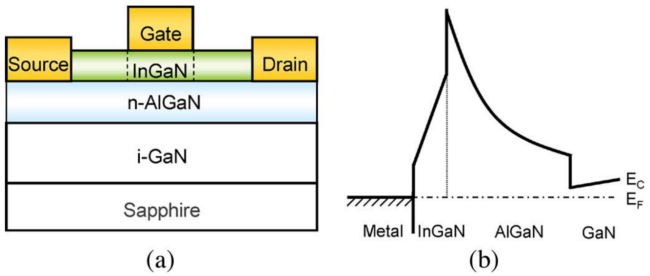

Figure 3.1: (a) Schematic diagram of polarization engineered InGaN/AlGaN/GaN HEMT and (b) its band diagram [17]

Fluoride Implantation

In this technique fluoride ions are introduced under the gate area using fluoride based plasma treatment or ion implantation [15]. Devices are subsequently annealed after gate deposition to mitigate the plasma damage. Negatively charged fluoride ions shift threshold voltage to positive values.

Gate Recessing

Normally-off operation can be achieved by using very thin AlGaN layer in an AlGaN/GaN heterostructure [19]. Gate recess method uses standard AlGaN/GaN het-

erostructure with thick AlGaN layer, where AlGaN is etched to very thin thickness to decrease 2DEG density in the channel. Etching only under the gate improves R_{ON}, because 2DEG channel in the access regions is unmodified [20].

AlGaN can be entirely etched creating so called "True-MOS" [21]. Threshold voltage should be more stable in such devices, but electron mobility is lower. Comparison between typical MISHEMT (metal insulator semiconductor HEMT) and True-MOS is depicted in Fig. 3.2.

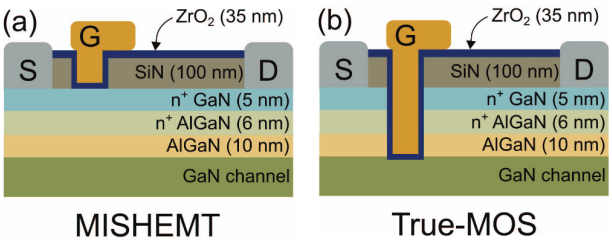

Figure 3.2: Schematic diagram MISHEMT (a) and True-MOS (b) [21].

p-GaN Gate

For a standard AlGaN/GaN heterostructures with Schottky gate, quantum well at the interface between AlGaN and GaN lies below Fermi level at 0 gate bias, which leads to normally-on operation. By adding p-GaN cap layer, presence of free holes raises the conduction band up to achieve normally-off operation [22]. Fig. 3.3 represents the principle of p-GaN/AlGaN/GaN device in comparison to AlGaN/GaN device.

3.2 Hole Channel Transistors

GaN-based transistors for various high-power and high frequency application are already well established [23]. However, there is still a need for a monolithic integration of power circuits with control circuits [24]. For that CMOS technology on GaN is needed. While the technology for the n-channel devices is relatively mature, p-channel devices still require major research effort to be comparable.

Hole channel without quantum well

There have been several attempts over the years to prepare MOSFETs with a pn junction consisting of p-GaN and n-GaN. Both p and n-channel devices were integrated

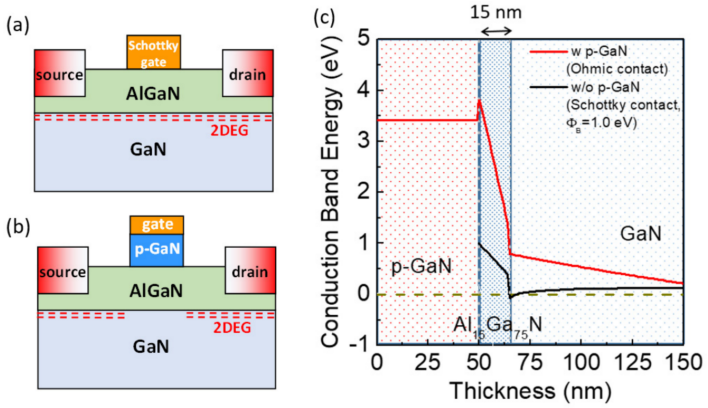

Figure 3.3: Schematic representation of (a) AlGaN/GaN HEMT with Schottky gate, (b) p-GaN/AlGaN/GaN HEMT with Schottky gate and (c) band diagrams of these heterostructures. P-GaN cap raises the conduction band up, leading to normally-off operation. Thickness of $Al_{0.15}Ga_{0.85}N$ thickness is 15 nm. Band diagram was simulated by commercially available Poisson solver [22].

on a single wafer [25]. Si was implanted under source and drain regions into p-type GaN for the n-channel device and additional Mg was implanted under the contacts for the p-channel device.

Inverted GaN/AlGaN/GaN heterostructure

In this approach, the heterostructure consists of GaN buffer, Al(In)GaN backbarrier and GaN channel. 2DEG is created at the bottom interface and 2DHG is created on the top interface. Al content in Al_xGa_{1-x} is usually around 0.4 [26], which is on a higher end of standard GaN HEMTs with Al molar fraction between 0.2 and 0.4 [27]. GaN channel should be doped with Mg to increase the valence band to allow for hole accumulation [28]. AlGaN might be replaced with InGaN [29], [30]. Schematic diagram of the heterostructure with corresponding band diagram is pictured in Fig. 3.4.

AlN/GaN platform

In this approach GaN is grown on a AlN buffer layer (Fig. 3.5). Due to polarization difference 2DHG is created at the interface. Mg doping is not necessary in this case. Hole mobility in the channel is $\sim$20 $cm^2V^{-1}s^{-1}$ at room temperature with a 2DHG sheet density of 5×10^{13} cm^{-2} [31].

Additional 2DEG channel can be produced by growing an additional AlN layer on

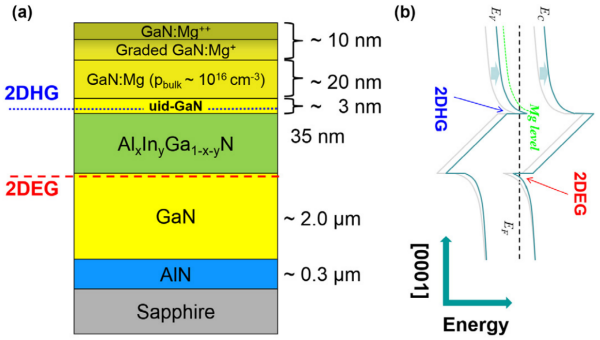

Figure 3.4: (a) Cross-section of a GaN/AlGaN/GaN heterostructure with 2DEG and 2DHG. (b) Simulated band diagram of the heterostructure with Mg doping in blue and without Mg doping in light gray color[28].

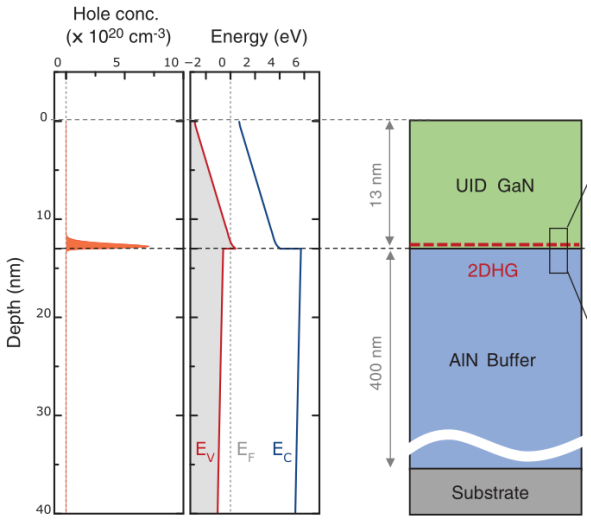

Figure 3.5: AlN/GaN heterostructure with a simulated band diagram [31]

top the GaN [32], with a possibility to grow 2DEG and 2DHG channel devices on the same wafer. Similarly to the GaN/AlGaN/GaN heterostructure, but reversed.

AlGaN/GaN superlatice

Hole channel devices have been prepared using p-AlGaN/p-GaN superlattices [33]. Sheet density in the hole channel was increased up to $\sim 5 \times 10^{13}$ cm^{-2} with moderate hole mobility of ~ 10 cm^{2}V^{-1}s^{-1}.

InAlN/GaN heterostructures

Another approach with non-inverted InAl(Ga)N/GaN, without parasitic 2DEG was proposed in recent paper [34]. $In_xAl_{1-x}N$ with $x \sim 0.17$ is lattice matched to GaN.

Further increase of x creates compressive strain in InAlN, which in turn generates piezoelectric polarization with opposite orientation to spontaneous polarization. In-rich InAlN with even higher $x > 0.32$ and piezoelectric polarization can reverse total polarization and create 2DHG at the interface. Comparison of GaN/AlGaN/GaN heterostructure with In-rich InAlN/GaN heterostructure is presented in Fig. 3.6.

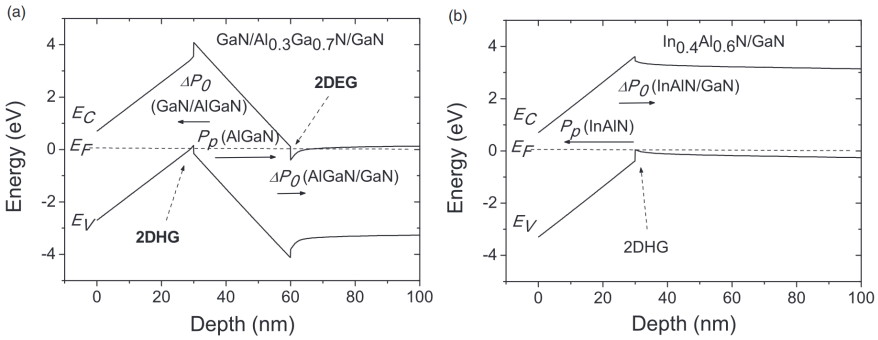

Figure 3.6: Band diagram of (a) GaN/AlGaN/GaN heterostructure and (b) InAlN/GaN heterostrocture simulated by 1D Schrödinger-Poisson solver. Adapted from [34].

Quaternary InAl(Ga)N instead of InAlN is proposed for two reasons. Al molar fraction is decreased by Ga, which in turn increases the polarization charge without the need to increase In molar fraction. Total polarization for $In_{0.3}Ga_xAl_{1-x}N$ is calculated in Fig. 3.7. Ga can be incorporated into the layer by a Ga memory effect [35], [36], which is usually negative effect, but in this case it is desired.

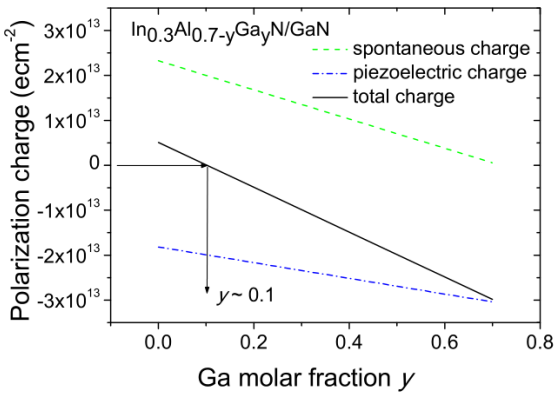

Figure 3.7: Calculated spontaneous, piezoelectric and total polarization for $In_{0.3}Ga_xAl_{1-x}N$.

This work will further explore this approach.

3.3 Mg Doping

In 2014, Nobel prize for physics was awarded to Isamu Akasaki, Hiroshi Amano and Shuji Nakamura "for the invention of efficient blue light-emitting diodes which has enabled bright and energy-saving white light sources" [37]. Manufacturing of blue LEDs is possible thanks to successful doping of GaN with Mg [38].

Mg remains the only viable candidate for p-type doping in GaN despite the relatively large activation energy 135-250 meV [39]–[42] compared to the activation energy of < 30 meV [43] for the n-type dopant Si.

During growth, Mg is incorporated into the layer in a form of stable and metastable electrically inactive Mg-H complexes [44]. Mg is then incorporated into the Ga position Mg_{Ga} by thermal treatment [45] from the metastable Mg-H complexes. Mg acts as an acceptor in this position. Only a few percent of all the Mg in the layer is electrically active (Fig. 3.8) [41].

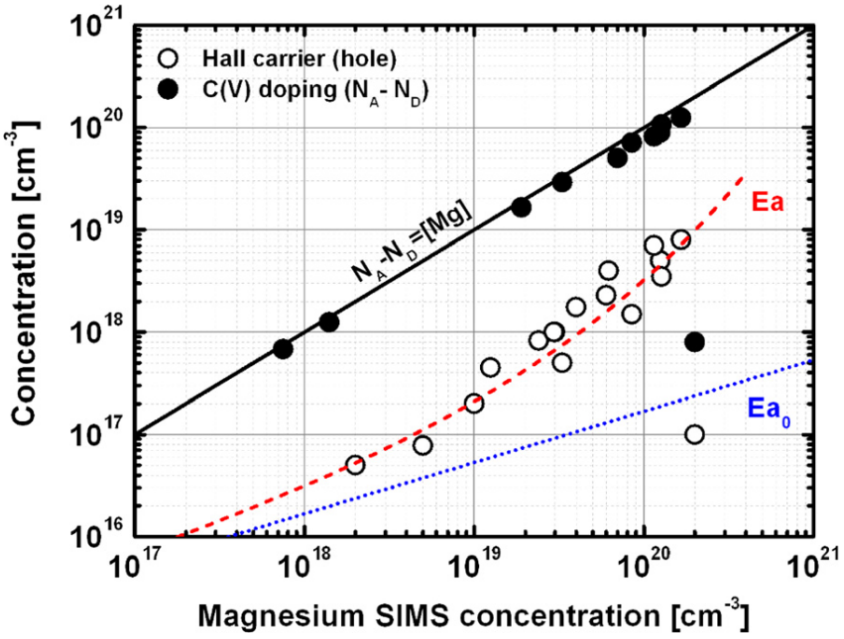

Figure 3.8: Hole density (open circles) and effective dopant concentration (full circles) as a function of Mg measured by SIMS. [41].

At higher Mg concentration of more than $\sim 10^{19}$ cm^{-3} selfcompensation takes effect, limiting the effective hole concentration even further. Mg acts as a double donor in interstitial position [46].

Acceptor concentration can be further improved by other techniques. Polarization

induced doping was used in [47] increase hole concentration by growing AlGaN with gradually increasing Al molar fraction. Hole concentration is increased by up to 5 orders of magnitude at low temperature compared to bulk p-GaN by growing AlGaN/GaN superlattice [48]. For the implanted Mg, ultra high pressure annealing at 1 GPa at 1673 K yielded 78% Mg activation [49].

Ohmic contacts on p-GaN are still under intense research as seen in several review papers [50], [51]. Ni/Au is usually used with annealing both in N_2 and O_2. Pt is sometimes used as it provides higher work function. Areas under contacts are sometimes overdoped with Mg to improve ohmic contact formation [52].

4 Material and Methods

Growth and processing

- **Metalorganic chemical vapor depostion (MOCVD)** - MOCVD is a method for deposition of single crystalline thin films. All samples in this work were grown by AIXTRON 3x2 CCS (Close coupled showerhead) system.

- **Processing** - All the samples were prepared using conventional processing techniques. Photolithography was performed using SUSS MicroTec MJB4 mask aligner with a UV-LED light source and AZ5214E photoresist. Mesa isolation was performed by reactive ion etching (RIE) in $SiCl_4$-based plasma in Oxford Plasmalab 100 Inductively Coupled Plasma (ICP). ICP was not used during the etching. Metal deposition was performed by e-beam evaporation in AJA Orion 8E. Indium contacts for Hall measurements were prepared by manually pressing $\sim$5 mm In spheres on the sample. Rapid thermal annealing (RTA) was performed in AnnealSys ASMicro.

Structural analysis

- **X-Ray Diffraction (XRD)** - XRD is an experimental technique used to determine the crystalline structure of a crystal

- **X-Ray Photoelectron Spectroscopy (XPS)** - XPS is a spectroscopy technique used to analyze the chemical analysis of the sample surface. It can detect atomic composition and detect chemical states of the atoms that are present on the surface.

- **Ultraviolet Photoelectron Spectroscopy (UPS)** - UPS is a similar method to XPS, except that ultraviolet light is used instead of X-rays. Because of lower photon energy, only valence electrons are emitted, but the energy is measured more precisely.

- **Auger Electron Spectroscopy (AES)** - AES is a surface-sensitive analytical technique used to investigate the elemental composition and chemical state of materials.

- **Secondary Ion Mass Spectroscopy (SIMS)** - SIMS is an analytical technique used for surface and depth profiling of materials.
- **Scanning Electron Microscopy (SEM)** - SEM is an imaging technique. It provides high-resolution imaging of sample surfaces using a focused beam of electrons.
- **Transmission Electron Microscopy (TEM)** - TEM is an imaging and analytical technique that provides detailed structural and compositional information at the atomic scale.
- **Atomic Force Microscopy (AFM)** - AFM is a powerful imaging and characterization technique used to investigate the topography, surface morphology, and physical properties of materials at the nanoscale.

Electrical characterization

- **Transfer length method (TLM)** - TLM is a technique used to determine sheet resistance of a semiconductor and contact resistance of the ohmic contact metalization.
- **Hall - Van Der Pauw** - Combination of Van der Pauw method and Hall effect is used to measure semiconductor resistivity, mobility and majority carrier concentration. Fig. 4.1 represents Hall measurement on a lower quality sample. Each color represents different combination of voltage and current polarities. Hall voltage difference between different magnetic fields is very small. For the black and red points simple analysis would yield a p-type sample. For the blue points, sample would be n-type. For the purple points, if we take into account only points at non-zero magnetic field, sample would be n-type. If we measured Hall voltage only at positive magnetic field, sample would be p-type and if we measured Hall voltage only at negative magnetic field sample would be n-type. Hall measurement on this sample is inconclusive. In the next chapters, when we mention Hall measurement was inconclusive, it means that something similar was measured as in Fig. 4.1.

- **Mercury Probe** - Mercury probe testing is a fast and nondestructive technique used to measure the electrical properties of semiconductor devices.
- **Measurement-stress-measurement (MSM)** - MSM technique is employed for the characterization of threshold voltage instabilities

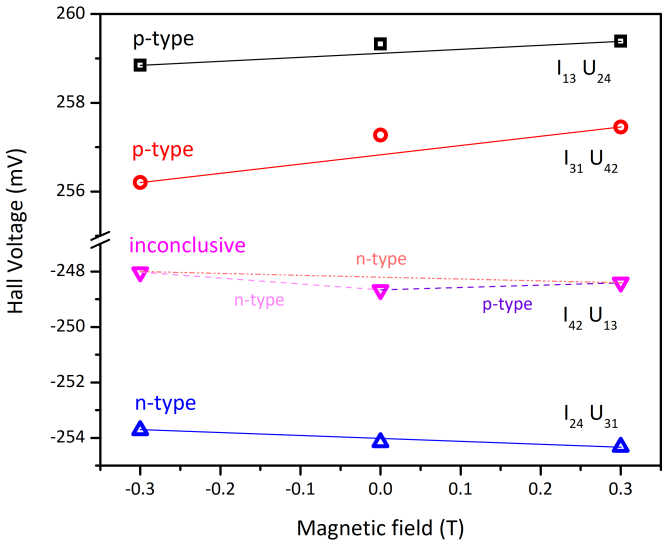

Figure 4.1: Example of a Hall measurement on a lower quality sample.

5 Results and discussion

5.1 Part I - Normally-off transistor with unintentional 2DHG

Results from this chapter were published in [53].

Previously our team has been developing normally-off transistors with various approaches [16], [18]. One of our approaches is to use a Al_2O_3/InGaN/AlGaN/GaN heterostructure (Fig. 5.1). In this approach high negative polarization at the InGaN/AlGaN interface is used to pull the conduction band up, depleting the 2DEG conductive channel. However, there is an additional unintentional 2DHG at the InGaN/AlGaN interface. This hole channel has a significant effect on the threshold voltage V_{TH} instabilities.

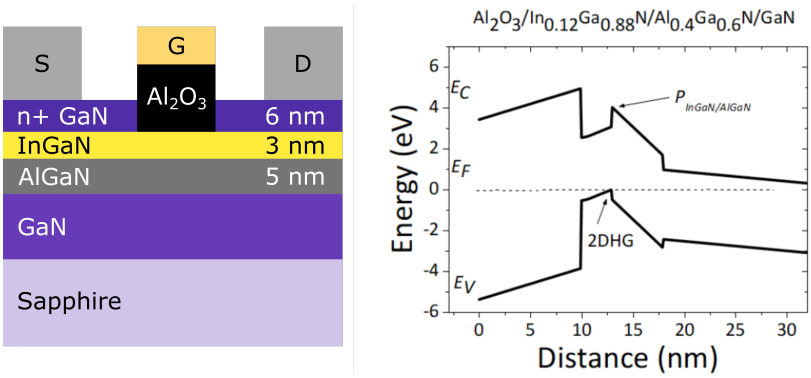

Figure 5.1: Schematic diagram of the cross-section of the prepared MOSHEMT (left) and simulated band diagram of the heterostructure under the gate (right).

The measured atomic percentages of the constituent atoms from XPS depth profiles correspond very well with the intended composition of 40% Al in the AlGaN layer and 12% In in the InGaN layer.

The evolution of the Ga2p3 binding energy peak (Fig. 5.2) in time provides additional insight into the valence band shape in the heterostructure. The Ga2p3 peak first rises with the etching time and then falls after 20 s of etching. This evolution of the binding energy corresponds very well with the shape of the valence band maximum in the calculated band diagram (Fig. 5.1) and could confirm the presence of the correct polarization charges in the heterostructure.

Transfer characteristics of the devices are presented in Fig. 5.3. Positive hysteresis of ∼0.5 V is apparent from Fig. 5.3a and b. There is a significant increase of the

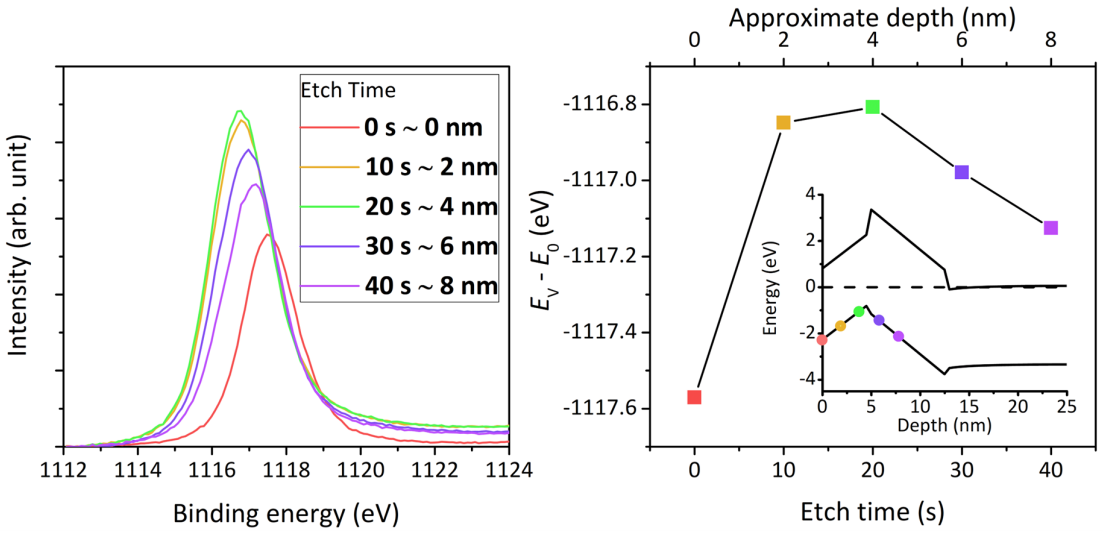

Figure 5.2: (a) XPS Ga2p3 spectra recorded at different etch times and (b) binding energy of each peak's maximum, plotted as energy difference from valence band. Inset depicts the band diagram without n+ GaN and Al_2O_3 with measurement depths highlighted. Etching rate is only approximate since it was calibrated for GaN layers. Peak shifts correspond to the calculated energy band diagram, confirming the presence of polarization charge.

gate current above $V_{GS} > 2$ V. This increase was found to be consistent with Fowler-Nordheim (FN) tunneling. Assuming effective mass of the tunneling electrons to be $m_{ox} = 0.75m_e$ [54], we calculated barrier height $\phi_B = 2.3eV$ and $\phi_B = 2.8eV$, depending on the fitted curve. Obtained tunneling barrier height is in good agreement with the Al_2O_3/InGaN conduction band offset of 2.4 eV assumed in the simulated band diagram [18].

Transfer characteristics in Fig. 5.3 exhibited an atypical threshold voltage shift, which was suspected to be the result of the 2DHG at the InGaN/AlGaN interface. Interface states have been shown to negatively impact the threshold voltage instabilities in MOSHEMTs [16], [55].

Measurement-stress-measurement technique [56] was employed to further analyze this behavior. In our experiments we used stress time T_{stress} from 0.1 s up to 50 s with a recovery time $T_{recovery}$ of 50 s. Stress voltage V_{stress} was 2.5 V and measurement voltage V_{meas} was 2 V.

Figure 5.4 [53] illustrates the observed drift of the threshold voltage (V_{TH}) on the measured sample. Threshold voltage V_{TH} shifts to positive values during stress. Then,

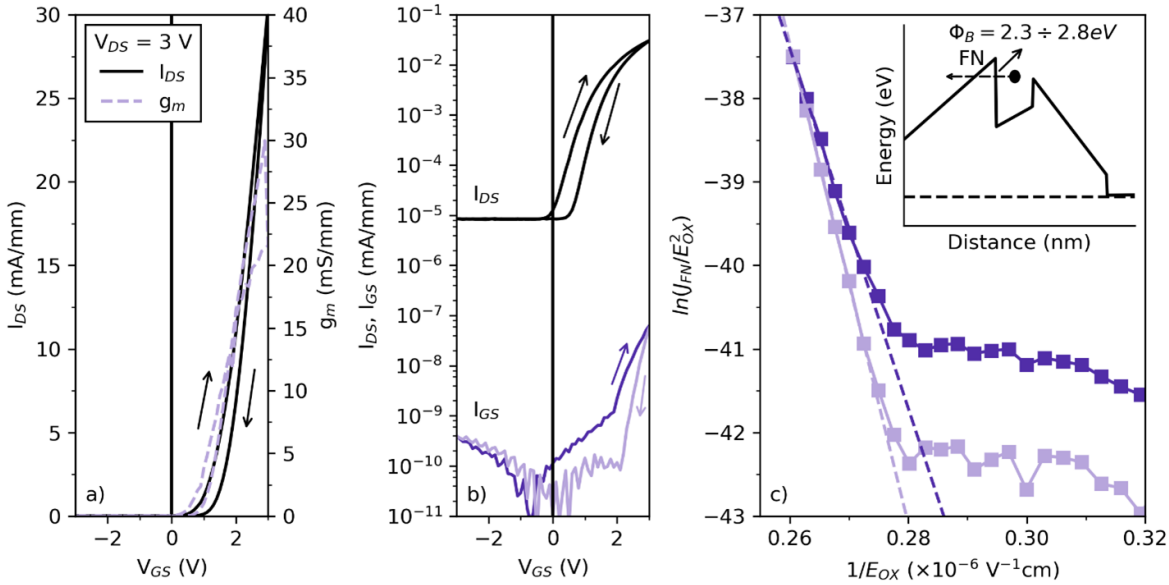

Figure 5.3: (a) Transfer and transconductance characteristic of a transistor, (b) Drain current and gate leakage current of a transistor in logarithmic scale, (c) Fowler-Nordheim plot, with a tunneling mechanism through Al_2O_3 oxide in an inset.

during recovery, V_{TH} shifts back to negative values, but ends beyond the starting value at even more negative V_{TH}. We propose a model where 2DHG plays an important role in the V_{TH} instability. Schematic representation of the capture and emission processes is presented in Fig. 5.5. In comparison to the normally-on device shown in Figure 2.3 from Chapter 2.3, the measured shift in V_{TH} was unexpected.

At thermal equilibrium 2DHG at the InGaN/AlGaN interface is filled with holes (Fig. 5.5a). There is no current flow between drain and source because 2DHG is depleted in the access regions because of the n+ GaN cap.

During stress, 2DEG at the AlGaN/GaN interface is populated with electrons. Electrons from 2DEG may be injected into InGaN. Interface traps at the Al_2O_3/InGaN interface that are now below Fermi level are filled with electrons. Holes in the InGaN remain even though 2DHG is below Fermi level, because of a large barrier on both sides (Fig. 5.5b).

Electrons and holes in InGaN may recombine and generate photon with an energy equivalent to the InGaN bandgap of ∼3 eV (Fig. 5.5c).

Generated photon may be reabsorbed by the interface trap, emitting an electron. Electron is emitted to the conduction band. From there it can tunnel through the triangular oxide barrier via Fowler-Norheim tunneling (Fig. 5.5d). FN tunneling was

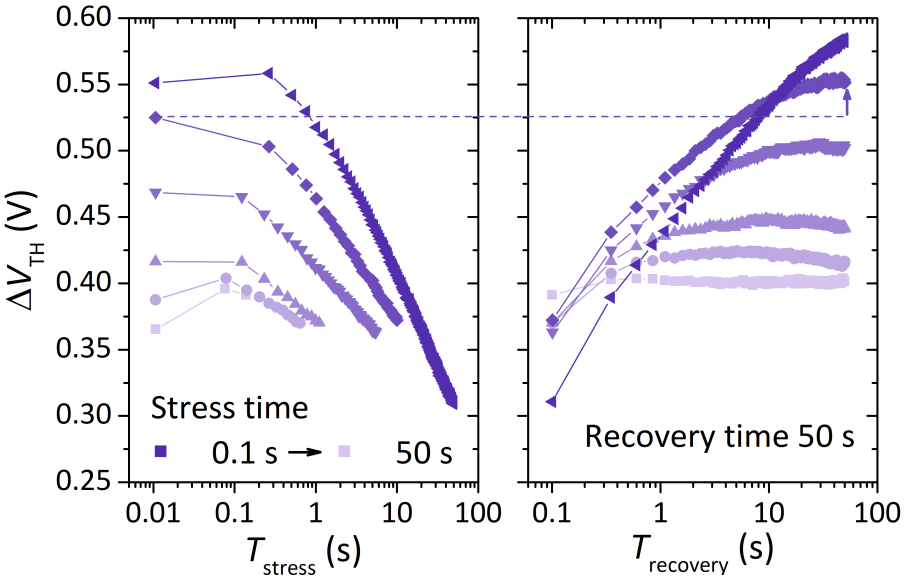

Figure 5.4: Threshold voltage V_{TH} drift in the normally-off Al_2O_3/InGaN/AlGaN/GaN MOSHEMT. Rising value of ΔV_{TH} means threshold voltage V_{TH} drifts towards positive values and vice versa [53].

observed on the IV curves in Fig. 5.3

Negative charge is removed from the gate stack by this process. V_{TH} should drift towards positive values, which was the observed behavior during stress period of the MSM measurement.

During recovery, gate stack returns to thermal equilibrium, but fewer holes remain in the 2DHG, increasing total negative charge in the gate stack (Fig. 5.5e). Some interface traps may still be filled with electrons, further increasing the negative charge. This would shift the threshold voltage V_{TH} towards negative values in comparison to the situation at the beginning of the measurement, which was again observed during MSM measurement.

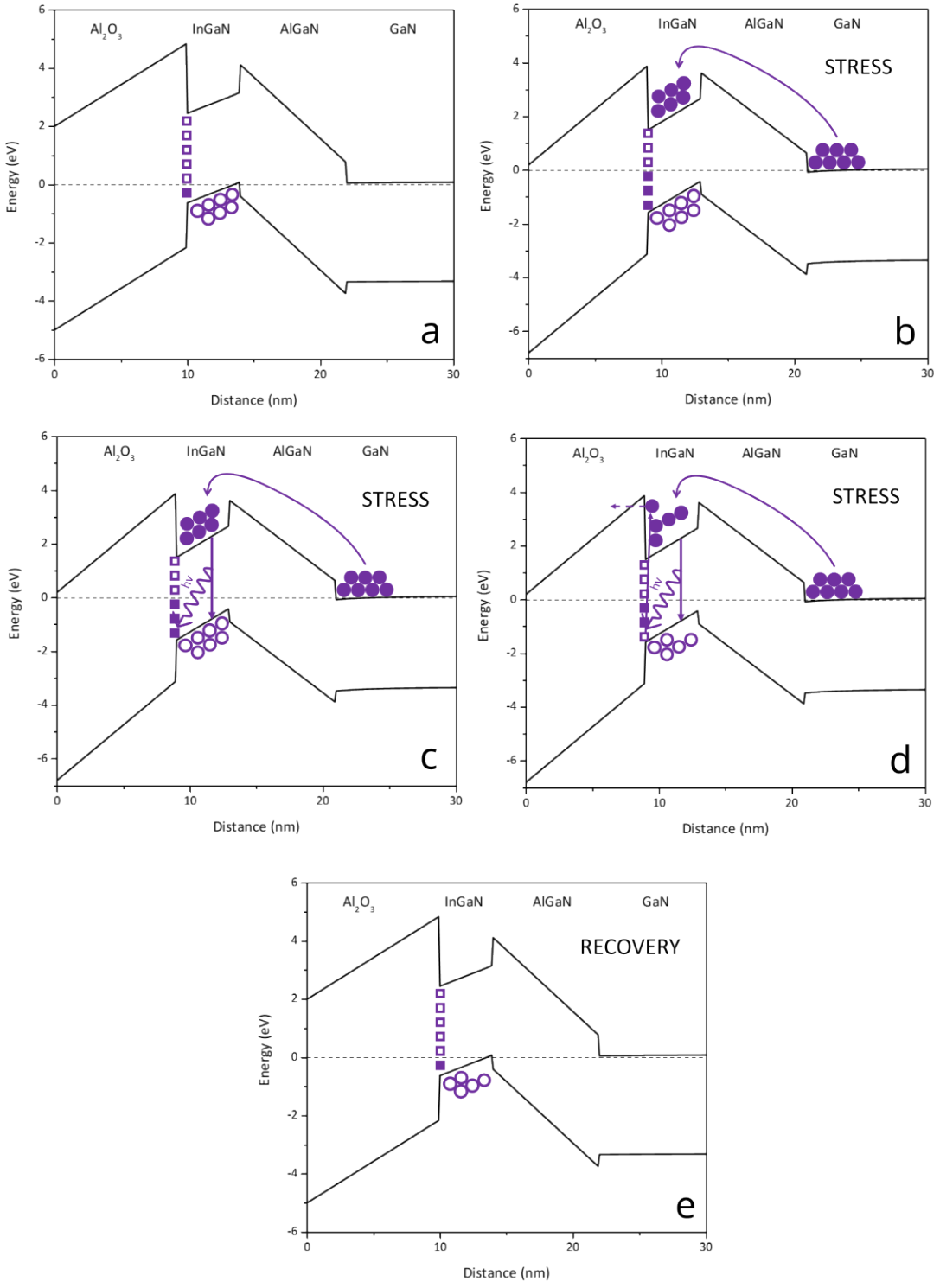

Figure 5.5: Simulated band diagram and various emission and capture processes that could be responsible for the measured threshold voltage drift. Band diagrams are simulated under the gate at (a) thermal equilibrium, (b), (c), (d) during stress at $V_{GS} > V_{TH}$ and (e) at the end of recovery at $V_{GS} = 0V$

5.2 Part II - InAlN/GaN hole channel

To create a transistor with a 2DHG we decided to further explore approach explained in chapter 3.2. In the paper [34] we proposed GaN/InAlN heterostructure with In content higher than 32%. For additional experiments, this was considered a reference sample MON 083. Sample MON 083 is an InAlN/GaN heterostructure grown on sapphire. To further improve our heterostructure we needed to decrease the thickness to increase the strain and to introduce Mg doping to increase the hole density in the quantum well.

Samples consisted of Al_2O_3 substrate, GaN buffer, InAl(Ga)N(:Mg) barrier layer and from later growths InGaN:Mg cap. Growth parameters of all the grown samples are listed in Tab. 1. Various modifications were perfomed: samples were thinned to increase strain, temperature was modified to optimize the In content, additional GaN channel layer was grown to improve InAlN/GaN interface.

Crystalline quality of the samples measured from XRD was not deteriorated as presented for samples MON227-MON234 in Fig. 5.6.

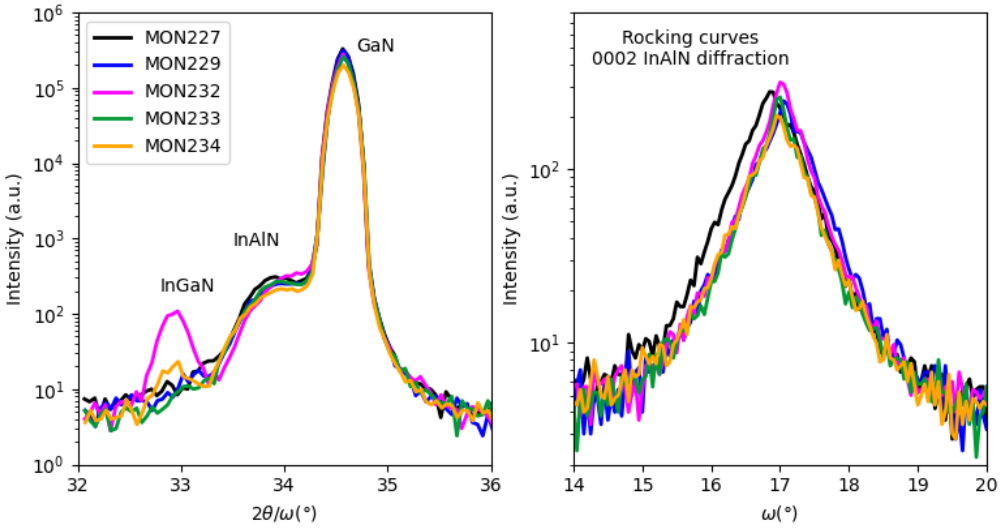

Figure 5.6: XRD spectra of samples MON 227, MON 229, MON 232, MON 233, MON 234. $2\theta/\omega$ scan on the left and rocking curve of the 0002 InAlN diffraction on the right.

In content should be sufficient to flip the total polarization charge as measured from the AES (Fig. 5.7).

For samples MON198-MON200, Fermi level was in the conduction band as mea-

Sample	InAlN thickness (nm)	InAlN growth temperature (°C)	Cp_2Mg flow (nmol/min)	InGaN thickness (nm)	InGaN growth temperature (°C)
MON 083	80	733	0	0	0
MON 198	65	737	260	0	0
MON 199	35	734	260	0	0
MON 200	35	734	50	0	0
MON 204	12	764	50	0	0
MON 205	11	764	260	0	0
MON 206	9	764	0	0	0
MON 208	7	765 → 830	0	0	0
MON 209	11	765 → 830	50	0	0
MON 210	12	765 → 830	260	0	0
MON 227	15	765	260	0	0
MON 229	12	765	260	2.5	720
MON 232	12	765	260	5	720
MON 233	12	765	260	2.5	737
MON 234	12	765	260	5	737
MON 238	12	750	50	0	0
MON 239	12	750	50	5	737

Table 1: Parameters of the growths.

sured from UPS (Fig. 5.8 and Fig 5.9)

Mg was present in the samples as measured by SIMS (Fig. 5.10). Mg concentration might be up to 10^{21} cm^{-3}.

Various ohmic contacts and contacts for Hall measurements were tested, however, hole conductivity was not measured in any of the samples.

Two other approaches (AlN/GaN and GaN/AlGaN/GaN) were also tested without success.

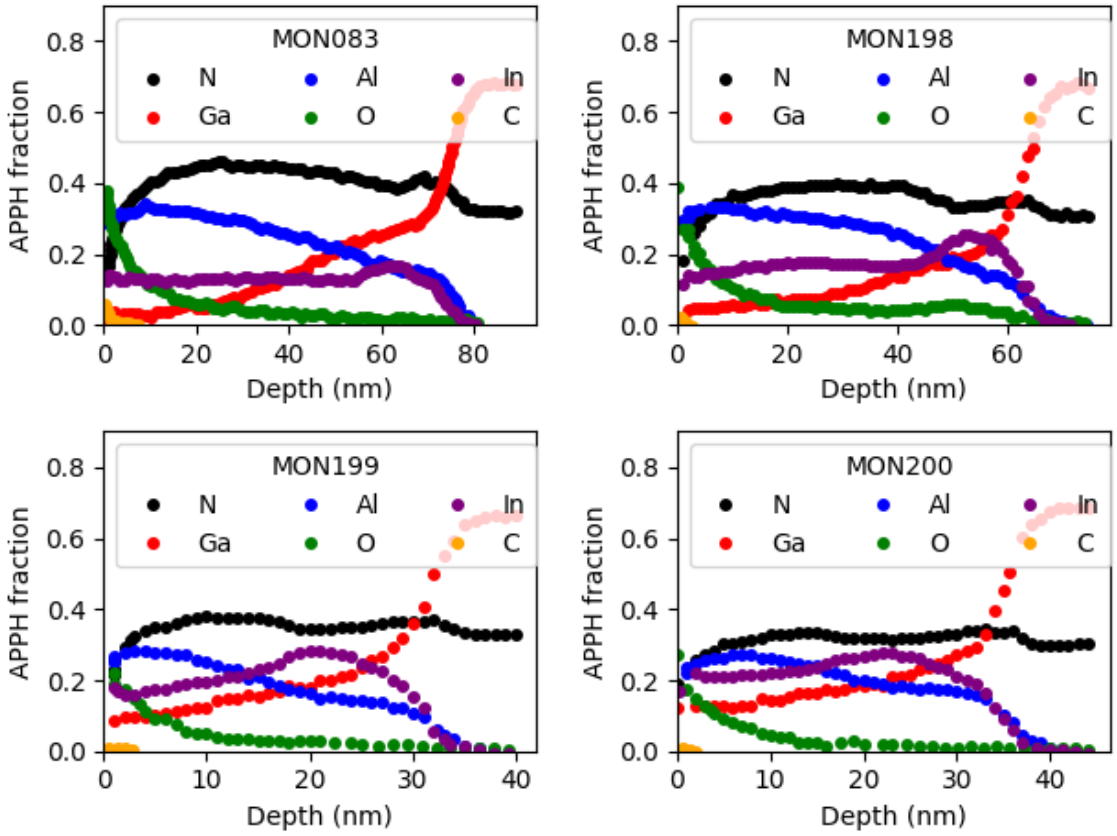

Figure 5.7: AES spectra of samples MON 083, MON 198, MON 199, MON 200.

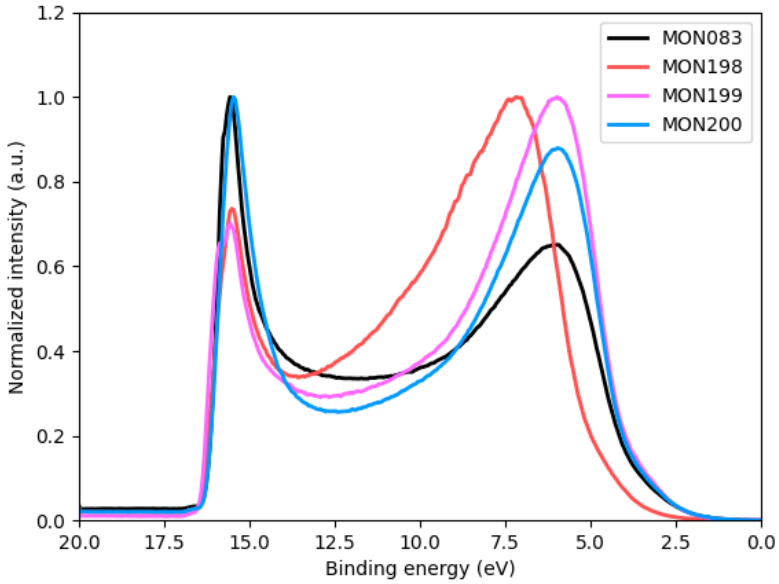

Figure 5.8: UPS spectra for samples MON 083, MON 198, MON 199, MON 200.

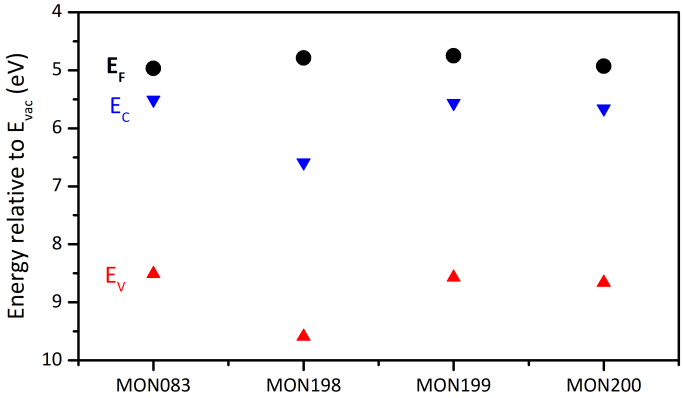

Figure 5.9: E_V (red), E_C (blue) and E_F (black) energy levels extracted from the UPS spectra.

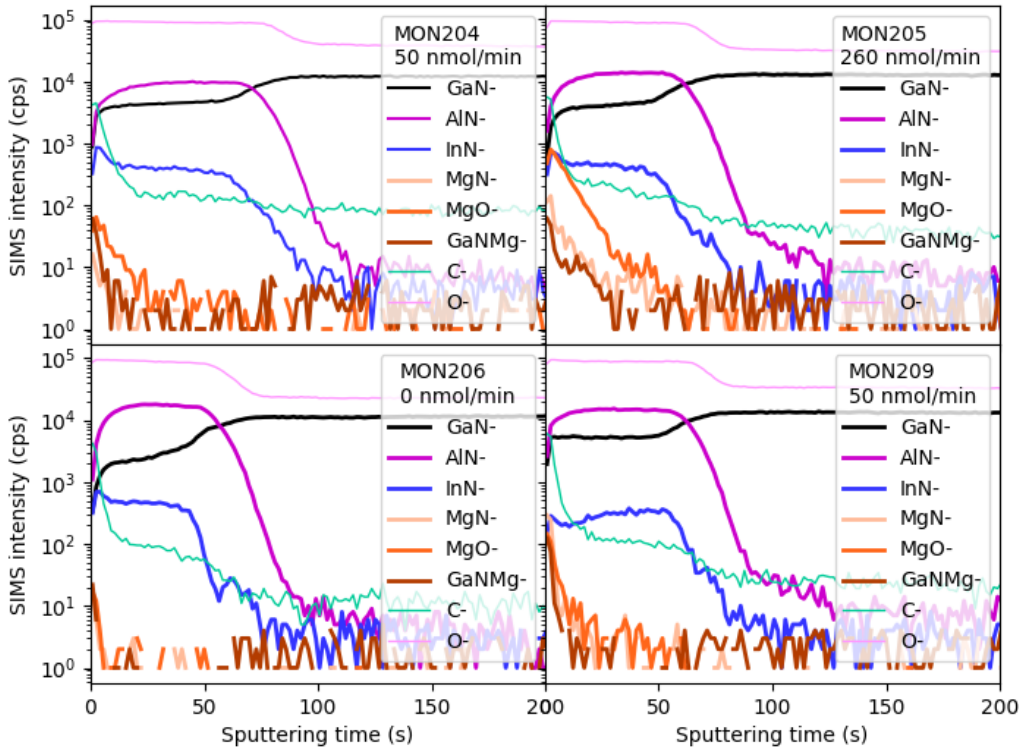

Figure 5.10: Selected secondary ions from SIMS spectra of samples MON 204, MON 205, MON 206 and MON 209.

5.3 Part III - Mg doping of In rich InAlN

Results from this chapter were published in [57].

Compared to the previous chapter, the aim was to grow a buffer layer for InN channel transistor. Because of its high electron velocity, InN might be a candidate for sub-THz electronics. MBE grown InN layers with a very high electron velocity were previously measured in [58].

Indium content in the buffer layer should be as high as possible to minimize mismatch between InAlN and InN. The buffer layer should be resistive so unintentional donors should be compensated, for example by acceptors from Mg doping.

The XRD analysis presented in Fig. 5.11 reveals that when the CP_2Mg flow was increased to 80 nmol/min, there was a noticeable shift towards higher angles in the (0002) diffraction of InAlN. This change was probably caused by a slight decrease in the In molar fraction (by up to 0.03). Additionally, the full width at half maximum (FWHM) of the signal increased, which was probably caused by the generation of additional screw and edge type dislocations. For the 260 nmol/min and 180 nmol/min CP_2Mg flow, an additional secondary peak was observed, indicating phase separation in the InAlN layer. Furthermore, a minor decrease in the growth rate was observed upon the introduction of Mg doping.

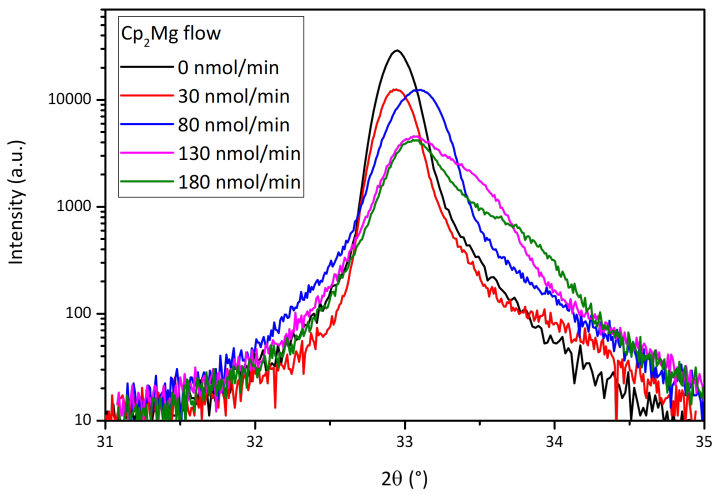

Figure 5.11: $2\theta/\omega$ scan of the (0002) diffraction of the InAlN layers with different Cp_2Mg flow.

The elemental SIMS profiles of the InAlN sample, doped with a CP_2Mg flow of 130 nmol/min, are presented in Fig. 5.12. MgO^- and MgN^- were detected with an almost constant intensity, providing a constant doping profile across the whole layer.

MgO^- rises significantly towards the surface, which was also observed in the previous chapter. SIMS calibration for the Mg ions was not performed, so extracting an atomic concentration of Mg is currently not possible from the measured data. GaN^- was not detected in the sample, so the reactor was sufficiently clear of the gallium from previous growths.

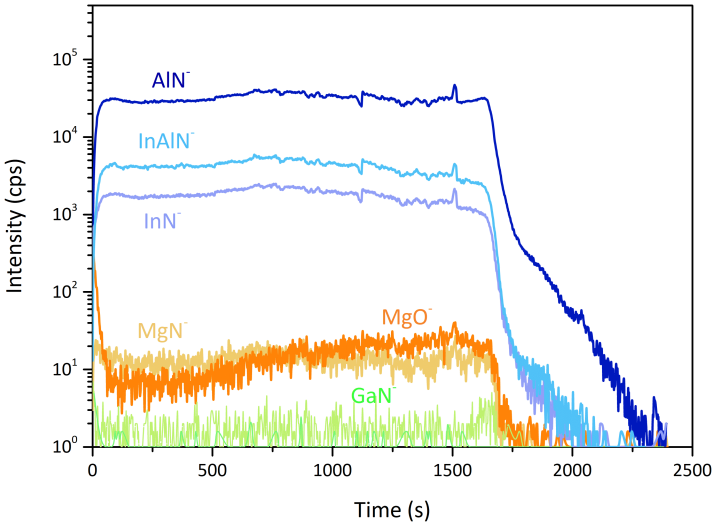

Figure 5.12: SIMS profile of a sample doped with a Cp_2Mg flow of 130 nmol/min.

A typical grain mosaic structure [59], [60] of undoped InAlN is shown in Fig. 5.13. A number of pits and surface roughness deterioration appeared with an increased Cp_2Mg flow of 30 nmol/min. Point defects disappeared as the flow of was further increased to 80 nmol/min in addition to enlargement of grains. Surface further deteriorated with higher Cp_2Mg flow and exhibited a number of misoriented grains.

Combining the results from XRD, AFM, SEM, and TEM analyses, it can be concluded that the microstructure of InAlN layers was improved by introducing a low Cp_2Mg flow, leading to fewer pits and suppressed growth of misoriented grains. However, the sample with the highest Cp_2Mg flow exhibited a high level of lattice disorder, accompanied by a loss of continuous "columnar" growth and the initiation of intense growth of conical grains with significant out-of-plane misorientation.

Photoluminescence (PL) was also measured, but a useful signal was obtained only from the undoped sample and the lowest doped sample. PL spectra are depicted in Fig. 5.14. PL maximum on the undoped sample of ∼1.71 eV correlated well with the

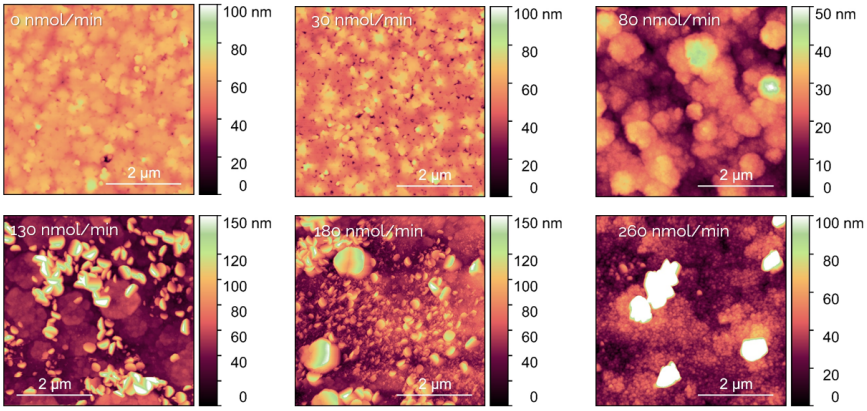

Figure 5.13: 5x5 µm AFM surface scans of InAlN layers with different Mg precursor flow.

In molar fraction extracted from the XRD measurements. For the doped sample peak shifted by ∼0.22 eV towards lower energies. FWHM of peak also increased from 258 meV to 466 meV. This might be correlated to the donor-acceptor pair reported for GaN in [61] and an effective band gap narrowing caused by defect-related potential fluctuations [62].

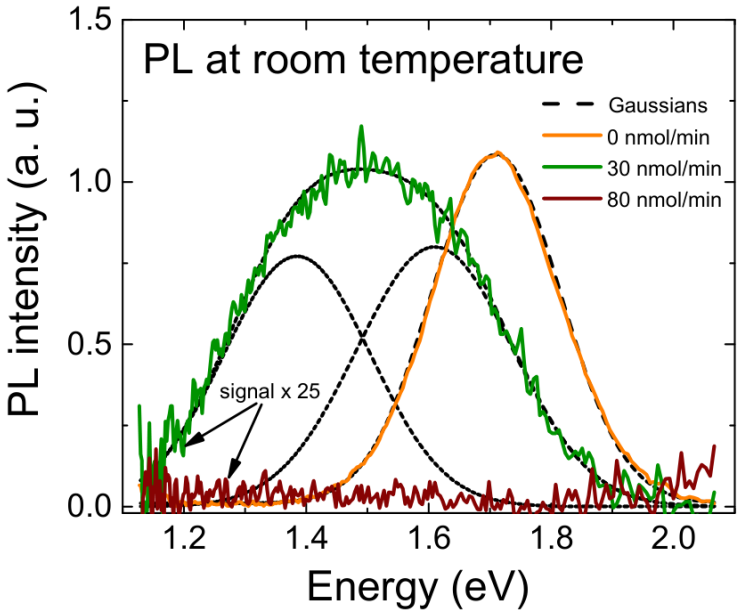

Figure 5.14: Room temperature PL spectra for the undoped InAlN sample and samples with two different Mg precursor flow rates.

Ti/Al/Ni/Au contacts were evaporated for TLM measurements. Contacts were not annealed, because we assume, that it will not be necessary for InN transistor. IV

curves were linear in the measurement range from -5 V to 5 V. Contact resistance and resistivity was extracted from the TLM measurements, the results are plotted in Fig. 5.15.

Resistivity increase by two orders of magnitude between undoped sample and sample grown at 80 nmol/min Mg precusor flow. At this point, resistivity starts to saturate. Contact resistance increased similarly, but contacts remained ohmic.

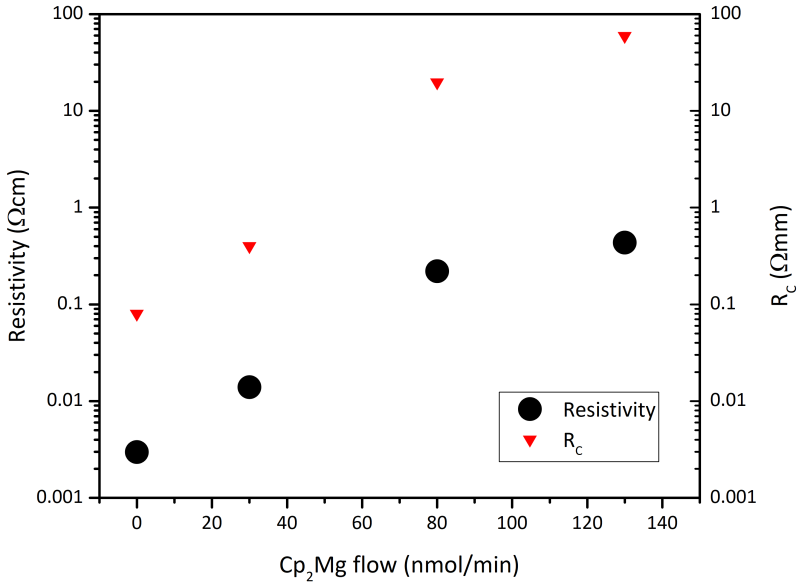

Figure 5.15: Contact resistance R_C and resistivity extracted from TLM measurements for samples with different Cp_2Mg flow.

Hall measurements were performed on the undoped sample, and two lowest doped samples from room temperature down to ∼4 K. Contacts were prepared in the Van der Pauw configuration. Resistivity, mobility and concentration was extracted from these measurements. The results are presented in Fig. 5.16

Similar to TLM measurements, resistivity increased by 2 orders of magnitude between undoped sample and sample grown with a Cp_2Mg flow rate of 80 nmol/min. Temperature dependencies along with mobilities and concentration provide additional insight into the mechanism of the resistivity increase.

For the undoped sample, resistivity is almost constant from ∼4 K up to room temperature. This suggests that the InAlN layer is degenerated with Fermi level in the conduction band. Upon closer inspection mobility rises until ∼150 K and then falls

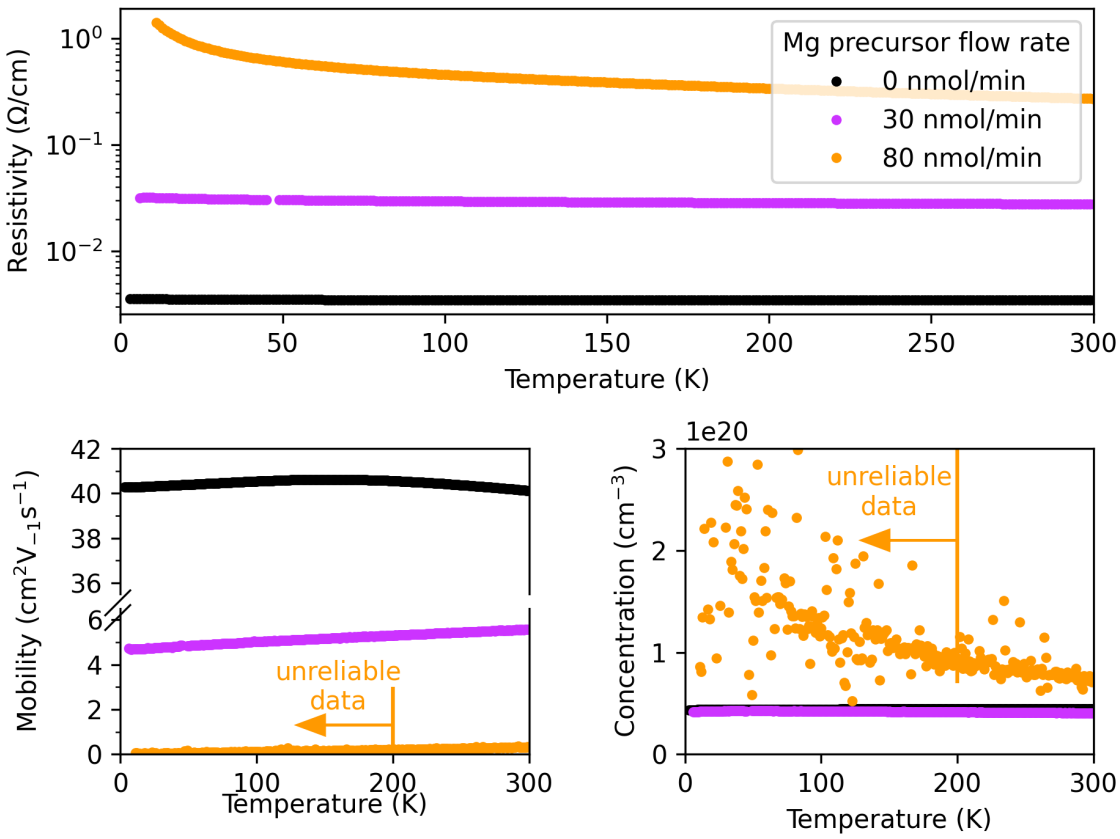

Figure 5.16: Resistivity, concentration and mobility extracted from Hall-Van der Pauw measurements on samples with 0, 30 and 80 nmol/min Mg precursor flow rate.

down towards 300 K. This might suggest scattering at ionized impurities at low temperature and scattering at dislocations at high temperatures. However, this dependence should follow $T^{3/2}$ at low temperature and $T^{-3/2}$. Mobility changes only from ∼40.1 to ∼40.6 $cm^2V^{-1}s^{-1}$, which might be too small, as the change is typically over several orders of magnitude. Mobility should also fall towards zero if we assume Brooks-Herring scattering at ionized impurities with a $T^{3/2}$ dependence, which is not the case here. Therefore, there might be some other mechanism that would cause the measured shape of the mobility. Concentration was very high around 4×10^{19} cm^{-3} and the sample was firmly n-type.

For the sample with a Cp_2Mg flow of 30 nmol/min, resistivity slightly increases towards 0 K. This change was caused by a decrease in mobility. Mobility does not fall down to 0, so this might still be considered a metal-like behaviour of a degenerated semiconductor. Compared to the undoped sample, mobility decreased from ∼40 $cm^2V^{-1}s^{-1}$ to ∼5 $cm^2V^{-1}s^{-1}$, which might be caused by defects introduced by Mg

doping. This was the cause of the resistivity decrease, because concentration remained almost the same with only 10% decrease compared to the undoped sample. Decrease in concentration might be an effect of a minor compensation by acceptors from Mg.

For the sample with a Cp_2Mg flow of 80 nmol/min, resistivity rises significantly towards 0 K. Mobility decreased well below 1 $cm^2V^{-1}s^{-1}$ and decreases with decreasing temperature, probably because of more defects introduced by additional Mg dopants. Concentration increased compared to previous samples, which might be caused by the amphoteric behavior of Mg at higher concentrations. Sample was still n-type. Note that data below 200 K for this sample might not be reliable, due to difficulty of measuring Hall on samples with very low mobility.

To summarize, resistivity increase of two orders of magnitude might be enough for a buffer layer in InN transistor. However, we see that even low Mg precursor flow rate has a detrimental effect on the mobility of the InAlN layers. Cp_2Mg flow rate of as low as 80 nmol/min decreases mobility to almost 0 $cm^2V^{-1}s^{-1}$. In the previous chapter we used a much higher flow rate of 260 nmol/min. Even the 50 nmol/min flow rate might be too high for the devices with hole channel, as that requires layers of good crystalline quality.

5.4 Summary and outlook

According to the paper published in 2019 [34], to prepare a hole channel InAlN/GaN transistor should have been relatively straightforward. Only Mg doping was necessary to improve hole density in the channel. However, we were not able to replicate any p-type conductivity in any of the other samples.

From the results in part III, which were measured only after all the experiments from part II, we see that Mg doping in quantities used in part II might be severely detrimental to the quality of the grown layers. Furthermore, from the UPS measurement, we have seen that Fermi level might be in the conduction band for much lower In content than ∼60% previously published in [63].

In the future, careful optimization of InAlN layer might be necessary to lower intrinsic electron concentration, as the 2DHG in the heterostructure should be formed even without Mg doping. Then Mg doping should be performed at much lower Cp_2Mg flows, which on the other might yield too low hole concentration, due to low activation.

After the presence of 2DHG would be confirmed, another issue may arise from ohmic contacts optimization. Standard metalization stacks and annealing in O_2 or N_2 might not be enough to prepare high quality ohmic contact. Selective area growth of Mg-doped GaN under the contacts might be necessary [64], to create overdoped layer to improve the ohmic contact formation. However, this would require optimization of SiN or some other passivation layer to serve as a mask during growth and optimization of Mg doping in GaN, which would probably need to be grown at low temperature due to low growth temperature of the InAlN layer.

Even with lower quality ohmic contacts, after achieving 2DHG, preparing a transistor should be achievable.

6 Conclusion

This work deals with hole channel GaN-based devices and hole type conductivity in these devices. Theoretical part provides an overview of experimental methods used in this thesis and a summary of the state of the art of the normally-off transistors and transistors with hole channel.

In the first part of the results, threshold voltage instabilities in the normally-off Al_2O_3/InGaN/AlGaN/GaN MOSHEMTs were investigated. Peculiar threshold voltage shift was measured in the opposite direction to the previously observed behavior on other AlGaN/GaN HEMTs. V_{TH} shift may have been caused by an unintentional 2DHG on the InGaN/AlGaN interface. We proposed a model that could explain this behavior. During stress, electrons may be injected into InGaN where they recombine with holes from 2DHG and generate photon. Photon may be reabsorbed at the oxide/InGaN interface states from where it emits electron into the conduction band. Electron can tunnel through triangular oxide barrier via Fowler-Nordheim tunneling, which was observed in the DC transfer characteristics. During recovery, some interface states might remain occupied and 2DHG might be partially depleted. This would explain both the positive V_{TH} shift during the stress and negative V_{TH} shift during the recovery.

InAl(Ga)N/GaN heterostructure with an intentional 2DHG was investigated in the second part of the results. Hole conductivity was not observed in any of the samples, so the results from the reference sample were not replicated. There are indications that Fermi level might be in the conduction band and that Mg precursor flow might be too high. Hall measurements were inconclusive, which might suggest very low mobility in all the samples.

Mg doping of In-rich InAlN layers was investigated in the third part of the thesis. Mg was used to increase resistivity by compensating intrinsic donors. Mg precursor flow was increased from 0 nmol/min up to 260 nmol/min. Resistivity of the samples increased by two orders of magnitude between undoped sample and sample with a Mg precursor flow of 80 nmol/min. Resistivity was increased by a decrease in mobility to almost 0 $cm^2V^{-1}s^{-1}$ caused by the defects introduced by the Mg doping. This might prove enough for a buffer layer in a transistor with InN channel.

InAlN layers severely degraded by Mg doping, which is an issue for the hole channel transistor where high quality layer is needed.

STU

List of Publications

Scientific papers in foreign journals registered in Current Contents Connect with IF (impacted) - ADCA

O. Pohorelec, M. Ťapajna, D. Gregušová, F. Gucmann, S. Hasenöhrl, Š. Haščík, R. Stoklas, A. Seifertová, B. Pécz, L. Tóth, and J. Kuzmík, "Investigation of interfaces and threshold voltage instabilities in normally-off MOS-gated InGaN/AlGaN/GaN HEMTs," *Applied Surface Science*, vol. 528, p. 146 824, Oct. 2020. DOI: 10.1016/j.apsusc.2020.146824

J. Kuzmík, O. Pohorelec, S. Hasenöhrl, M. Blaho, R. Stoklas, E. Dobročka, A. Rosová, M. Kučera, F. Gucmann, D. Gregušová, M. Precner, and A. Vincze, "Mg Doping of N-Polar, In-Rich InAlN," *Materials*, vol. 16, no. 6, p. 2250, Mar. 2023. DOI: 10.3390/ma16062250

D. Gregušová, L. Tóth, O. Pohorelec, S. Hasenöhrl, Š. Haščík, I. Cora, Z. Fogarassy, R. Stoklas, A. Seifertová, M. Blaho, A. Laurenčíková, T. Oyobiki, B. Pécz, T. Hashizume, and J. Kuzmík, "InGaN/(GaN)/AlGaN/GaN normally-off metal-oxide-semiconductor high-electron mobility transistors with etched access region," *Japanese Journal of Applied Physics*, vol. 58, no. SC, SCCD21, Jun. 2019. DOI: 10.7567/1347-4065/ab06b8

F. Gucmann, M. Ťapajna, O. Pohorelec, Š. Haščík, K. Hušeková, and J. Kuzmík, "Creation of Two-Dimensional Electron Gas and Role of Surface Donors in III-N Metal-Oxide-Semiconductor High-Electron Mobility Transistors," *physica status solidi (a)*, vol. 215, no. 24, p. 1 800 090, Dec. 2018. DOI: 10.1002/pssa.201800090

R. Kúdela, J. Šoltýs, M. Kučera, R. Stoklas, F. Gucmann, M. Blaho, M. Mičušík,

O. Pohorelec, M. Gregor, I. Brytavskyi, E. Dobročka, and D. Gregušová, "Technology and application of in-situ AlOx layers on III-V semiconductors," *Applied Surface Science*, vol. 461, pp. 33–38, Dec. 2018. DOI: 10.1016/j.apsusc.2018.06.229

D. Gregušová, E. Dobročka, P. Eliáš, R. Stoklas, M. Blaho, O. Pohorelec, Š. Haščík, M. Kučera, and R. Kúdela, "GaAs Nanomembranes in the High Electron Mobility Transistor Technology," *Materials*, vol. 14, no. 13, p. 3461, Jun. 2021. DOI: 10.3390/ma14133461

Scientific papers in foreign non-impacted journals registered in Web of Sciences or Scopus - ADMB

F. Gucmann, D. Gregusova, L. Valik, M. Tapajna, S. Hascik, K. Husekova, K. Frohlich, O. Pohorelec, and J. Kuzmik, "DC and pulsed IV characterisation of AlGaN/GaN MOS-HEMT structures with Al_2O_3 gate dielectric prepared by various techniques," in *2016 11th International Conference on Advanced Semiconductor Devices & Microsystems (ASDAM)*, IEEE, Nov. 2016. DOI: 10.1109/asdam.2016.7805883

M. Tapajna, K. Husekova, O. Pohorelec, L. Valik, S. Hascik, F. Gucmann, K. Frohlich, D. Gregusova, and J. Kuzmik, "Effect of HCl pretreatment on the oxide/semiconductor interface state density in AlGaN/GaN MOS-HEMT structures with MOCVD grown $A1_2O_3$ gate dielectric," in *2016 11th International Conference on Advanced Semiconductor Devices & Microsystems (ASDAM)*, IEEE, Nov. 2016. DOI: 10.1109/asdam.2016.7805931

Published invited papers from foreign scientific conferences - AFA

D. Gregušová, M. Blaho, O. Pohorelec, R. Stoklas, P. Eliáš, E. Dobročka, and R. Kúdela, "GaAs nanomembranes in device technology," in *SURFINT - SREN IV 2019*, Slovakia: Comenius University Bratislava, Jan. 2019, pp. 136–137, ISBN: 978-80-223-4811-9

D. Gregušová, O. Pohorelec, M. Ťapajna, M. Blaho, F. Gucmann, R. Stoklas, S. Hasenöhrl, A. Laurenčíková, P. Šichman, Š. Haščík, and J. Kuzmík, "Polarization engineering in GaN-based devices," in *2021 International Meeting for Future of Electron Devices*, Kansai: IEEE, Jan. 2021, pp. 1–4, ISBN: 978-1-6654-4200-8

Published papers from foreign scientific conferences - AFC

O. Pohorelec, M. Ťapajna, D. Gregušová, S. Hasenöhrl, Š. Haščík, R. Stoklas, K. Frohlich, B. Pécz, L. Tóth, and J. Kuzmík, "Investigation of interfaces and threshold voltage instabilities in MOS-gated InGaN/AlGaN/GaN HEMTs," in *SURFINT – SREN IV 2019*, Slovakia: Comenius University Bratislava, Jan. 2019, pp. 136–137, ISBN: 978-80-223-4811-9

O. Pohorelec, S. Hasenöhrl, M. Blaho, R. Stoklas, E. Dobročka, P. Nádaždy, A. Vincze, P. Eliáš, M. Kučera, F. Gucmann, D. Gregušová, and J. Kuzmík, "Mg doping in In-rich InAlN layers," in *2022 International Workshop on Nitride Semiconductors*, Germany: IWN2022, Jan. 2022, p. 255

Published papers from domestic scientific conferences - AFD

O. Pohorelec, M. Ťapajna, D. Gregušová, K. Frohlich, and J. Kuzmík, "Investigation of threshold voltage instabilities in MOS-gated InGaN/AlGaN/GaN HEMTs," in

ADEPT 2019 : 7th International Conference on Advances in Electronic and Photonic Technologies, Slovakia: University of Žilina, Jan. 2019, pp. 123–126, ISBN: 978-80-554-1568-0

M. Ťapajna, F. Egyenes, S. Hasenöhrl, M. Blaho, O. Pohorelec, A. Vincze, M. Muška, P. Noga, and D. Gregušová, "Investigation of GaN P-N junction processed by Mg ion implantation," in *ADEPT 2019 : 7th International Conference on Advances in Electronic and Photonic Technologies*, Slovakia: University of Žilina, Jan. 2019, ISBN: 978-80-554-1568-0

O. Pohorelec, D. Gregušová, S. Hasenöhrl, E. Dobročka, R. Stoklas, Ľ. Vančo, M. Gregor, and J. Kuzmík, "Mg doping of InAlN layers," in *ADEPT 2021 : 9th International Conference on Advances in Electronic and Photonic Technologies*, Slovakia: Univ. Zilina in EDIS-Publishing Centre of UZ, Jan. 2021, pp. 147–150, ISBN: 978-80-554-1806-3

References

[1] Yole Group. "China's lead in power GaN consumer devices drives the future use in telecom/datacom and automotive." (Mar. 2023), [Online]. Available: https://www.yolegroup.com/strategy-insights/chinas-lead-in-power-gan-consumer-devices-drives-the-future-use-in-telecom-datacom-and-automotive/.

[2] Qorvo. "Why GaN is 5G's Super 'Power'." (Mar. 2021), [Online]. Available: https://www.qorvo.com/design-hub/blog/why-gan-is-5g-super-power.

[3] R. Brown, "A novel AlGaN/GaN based enhancement-mode high electron mobility transistor with sub-critical barrier thickness.," Ph.D. dissertation, University of Glasgow, Jan. 2015.

[4] J. Kuzmik, A. Kostopoulos, G. Konstantinidis, J.-F. Carlin, A. Georgakilas, and D. Pogany, "InAlN/GaN HEMTs: A first insight into technological optimization," *IEEE Transactions on Electron Devices*, vol. 53, no. 3, pp. 422–426, Mar. 2006. DOI: 10.1109/ted.2005.864379. [Online]. Available: https://doi.org/10.1109/ted.2005.864379.

[5] K. Jeganathan, M. Shimizu, H. Okumura, Y. Yano, and N. Akutsu, "Lattice-matched InAlN/GaN two-dimensional electron gas with high mobility and sheet carrier density by plasma-assisted molecular beam epitaxy," *Journal of Crystal Growth*, vol. 304, no. 2, pp. 342–345, Jun. 2007. DOI: 10.1016/j.jcrysgro.2007.03.035. [Online]. Available: https://doi.org/10.1016/j.jcrysgro.2007.03.035.

[6] P. Cui and Y. Zeng, "Scaling behavior of InAlN/GaN HEMTs on silicon for RF applications," *Scientific Reports*, vol. 12, no. 1, Oct. 2022. DOI: 10.1038/s41598-022-21092-9. [Online]. Available: https://doi.org/10.1038/s41598-022-21092-9.

[7] J. Kuzm k, "InAlN/(In)GaN high electron mobility transistors: Some aspects of the quantum well heterostructure proposal," *Semiconductor Science and Technology*, vol. 17, no. 6, pp. 540–544, Jun. 2002. DOI: 10.1088/0268-1242/17/6/307. [Online]. Available: https://doi.org/10.1088/0268-1242/17/6/307.

[8] M. Stutzmann, O. Ambacher, M. Eickhoff, *et al.*, "Playing with Polarity," *physica status solidi (b)*, vol. 228, no. 2, pp. 505–512, Nov. 2001. DOI: 10.1002/1521-3951(200111)228:2<505::aid-pssb505>3.0.co;2-u. [Online]. Available: https://doi.org/10.1002/1521-3951%28200111%29228%3A2%3C505%3A%3Aaid-pssb505%3E3.0.co%3B2-u.

[9] O. Ambacher, J. Smart, J. R. Shealy, *et al.*, "Two-dimensional electron gases induced by spontaneous and piezoelectric polarization charges in N- and Ga-face AlGaN/GaN heterostructures," *Journal of Applied Physics*, vol. 85, no. 6, pp. 3222–3233, Mar. 1999. DOI: 10.1063/1.369664. [Online]. Available: https://doi.org/10.1063/1.369664.

[10] M. Ťapajna, "Current Understanding of Bias-Temperature Instabilities in GaN MIS Transistors for Power Switching Applications," *Crystals*, vol. 10, no. 12, p. 1153, Dec. 2020. DOI: 10.3390/cryst10121153. [Online]. Available: https://doi.org/10.3390/cryst10121153.

[11] M. Blaho, D. Gregušová, Š. Haščík, *et al.*, "Technology of integrated self-aligned E/D-mode n^{++}GaN/InAlN/AlN/GaN MOS HEMTs for mixed-signal electronics," *Semiconductor Science and Technology*, vol. 31, no. 6, p. 065 011, Jun. 2016. DOI: 10.1088/0268-1242/31/6/065011. [Online]. Available: https://doi.org/10.1088/0268-1242/31/6/065011.

[12] T. Palacios, C.-S. Suh, A. Chakraborty, S. Keller, S. DenBaars, and U. Mishra, "High-performance E-mode AlGaN/GaN HEMTs," *IEEE Electron Device Letters*, vol. 27, no. 6, pp. 428–430, Jun. 2006. DOI: 10.1109/led.2006.874761. [Online]. Available: https://doi.org/10.1109/led.2006.874761.

[13] O. Hilt, E. Bahat-Treidel, A. Knauer, F. Brunner, R. Zhytnytska, and J. Würfl, "High-voltage normally OFF GaN power transistors on SiC and Si substrates," *MRS Bulletin*, vol. 40, no. 5, pp. 418–424, May 2015. DOI: 10.1557/mrs.2015.88. [Online]. Available: https://doi.org/10.1557/mrs.2015.88.

[14] C.-T. Chang, T.-H. Hsu, E. Chang, Y.-C. Chen, H.-D. Trinh, and K. Chen, "Normally-off operation AlGaN/GaN MOS-HEMT with high threshold voltage," *Electronics Letters*, vol. 46, no. 18, p. 1280, Jan. 2010. DOI: 10.1049/el.2010.1939. [Online]. Available: https://doi.org/10.1049/el.2010.1939.

[15] Yong Cai, Yugang Zhou, K. Chen, and K. Lau, "High-performance enhancement-mode AlGaN/GaN HEMTs using fluoride-based plasma treatment," *IEEE Electron Device Letters*, vol. 26, no. 7, pp. 435–437, Jul. 2005. DOI: 10.1109/led.2005.851122. [Online]. Available: https://doi.org/10.1109/led.2005.851122.

[16] M. Ťapajna and J. Kuzmík, "Control of Threshold Voltage in GaN Based Metal–Oxide–Semiconductor High-Electron Mobility Transistors towards the Normally-Off Operation," *Japanese Journal of Applied Physics*, vol. 52, no. 8S, 08JN08, Aug. 2013. DOI: 10.7567/jjap.52.08jn08. [Online]. Available: https://doi.org/10.7567/jjap.52.08jn08.

[17] T. Mizutani, M. Ito, S. Kishimoto, and F. Nakamura, "AlGaN/GaN HEMTs With Thin InGaN Cap Layer for Normally Off Operation," *IEEE Electron Device Letters*, vol. 28, no. 7, pp. 549–551, Jul. 2007. DOI: 10.1109/led.2007.900202. [Online]. Available: https://doi.org/10.1109/led.2007.900202.

[18] D. Gregušová, M. Blaho, Š. Haščík, *et al.*, "Polarization-Engineered n^+ GaN/InGaN/AlGaN/GaN Normally-Off MOS HEMTs," *physica status solidi (a)*, vol. 214, no. 11, p. 1 700 407, Nov. 2017. DOI: 10.1002/pssa.201700407. [Online]. Available: https://doi.org/10.1002/pssa.201700407.

[19] M. A. Khan, Q. Chen, C. J. Sun, *et al.*, "Enhancement and depletion mode GaN/AlGaN heterostructure field effect transistors," *Applied Physics Letters*, vol. 68, no. 4, pp. 514–516, Jan. 1996. DOI: 10.1063/1.116384. [Online]. Available: https://doi.org/10.1063/1.116384.

[20] W. Saito, Y. Takada, M. Kuraguchi, K. Tsuda, and I. Omura, "Recessed-gate structure approach toward normally off high-Voltage AlGaN/GaN HEMT for power electronics applications," *IEEE Transactions on Electron Devices*, vol. 53, no. 2, pp. 356–362, Feb. 2006. DOI: 10.1109/ted.2005.862708. [Online]. Available: https://doi.org/10.1109/ted.2005.862708.

[21] M. Capriotti, C. Fleury, O. Bethge, *et al.*, "E-mode AlGaN/GaN True-MOS, with high-k ZrO_2 gate insulator," in *ESSDERC 2015 - 45th European Solid-State Device Research Conference*, IEEE, Sep. 2015. DOI: 10.1109/essderc.2015.

7324713. [Online]. Available: https://doi.org/10.1109/essderc.2015.7324713.

[22] F. Roccaforte, G. Greco, P. Fiorenza, and F. Iucolano, "An Overview of Normally-Off GaN-Based High Electron Mobility Transistors," *Materials*, vol. 12, no. 10, p. 1599, May 2019. DOI: 10.3390/ma12101599. [Online]. Available: https://doi.org/10.3390/ma12101599.

[23] H. Amano, Y. Baines, E. Beam, *et al.*, "The 2018 GaN power electronics roadmap," *Journal of Physics D: Applied Physics*, vol. 51, no. 16, p. 163 001, Apr. 2018. DOI: 10.1088/1361-6463/aaaf9d. [Online]. Available: https://doi.org/10.1088/1361-6463/aaaf9d.

[24] S. J. Bader, H. Lee, R. Chaudhuri, *et al.*, "Prospects for Wide Bandgap and Ultrawide Bandgap CMOS Devices," *IEEE Transactions on Electron Devices*, vol. 67, no. 10, pp. 4010–4020, Oct. 2020. DOI: 10.1109/ted.2020.3010471. [Online]. Available: https://doi.org/10.1109/ted.2020.3010471.

[25] N. H. Trung, N. Taoka, H. Yamada, T. Takahashi, T. Yamada, and M. Shimizu, "Experimental Demonstration of n- and p-channel GaN-MOSFETs toward Power IC Applications," *ECS Journal of Solid State Science and Technology*, vol. 9, no. 1, p. 015 001, Jan. 2020. DOI: 10.1149/2.0012001jss. [Online]. Available: https://doi.org/10.1149/2.0012001jss.

[26] M. Shatalov, G. Simin, Jianping Zhang, *et al.*, "GaN/AlGaN p-channel inverted heterostructure JFET," *IEEE Electron Device Letters*, vol. 23, no. 8, pp. 452–454, Aug. 2002. DOI: 10.1109/led.2002.801295. [Online]. Available: https://doi.org/10.1109/led.2002.801295.

[27] M. Meneghini, C. De Santi, I. Abid, *et al.*, "GaN-based power devices: Physics, reliability, and perspectives," *Journal of Applied Physics*, vol. 130, no. 18, p. 181 101, Nov. 2021. DOI: 10.1063/5.0061354. [Online]. Available: https://doi.org/10.1063/5.0061354.

[28] B. Reuters, H. Hahn, A. Pooth, *et al.*, "Fabrication of p-channel heterostructure field effect transistors with polarization-induced two-dimensional hole gases at metal–polar GaN/AlInGaN interfaces," *Journal of Physics D: Applied Physics*,

vol. 47, no. 17, p. 175 103, Apr. 2014. DOI: 10.1088/0022-3727/47/17/175103. [Online]. Available: https://doi.org/10.1088/0022-3727/47/17/175103.

[29] T. Zimmermann, M. Neuburger, M. Kunze, *et al.*, "P-Channel InGaN-HFET Structure Based on Polarization Doping," *IEEE Electron Device Letters*, vol. 25, no. 7, pp. 450–452, Jul. 2004. DOI: 10.1109/led.2004.830285. [Online]. Available: https://doi.org/10.1109/led.2004.830285.

[30] K. Zhang, M. Sumiya, M. Liao, Y. Koide, and L. Sang, "P-Channel InGaN/GaN heterostructure metal-oxide-semiconductor field effect transistor based on polarization-induced two-dimensional hole gas," *Scientific Reports*, vol. 6, no. 1, Mar. 2016. DOI: 10.1038/srep23683. [Online]. Available: https://doi.org/10.1038/srep23683.

[31] R. Chaudhuri, S. J. Bader, Z. Chen, D. A. Muller, H. G. Xing, and D. Jena, "A polarization-induced 2D hole gas in undoped gallium nitride quantum wells," *Science*, vol. 365, no. 6460, pp. 1454–1457, Sep. 2019. DOI: 10.1126/science.aau8623.

[32] A. Hickman, R. Chaudhuri, S. J. Bader, *et al.*, "High Breakdown Voltage in RF AlN/GaN/AlN Quantum Well HEMTs," *IEEE Electron Device Letters*, vol. 40, no. 8, pp. 1293–1296, Aug. 2019. DOI: 10.1109/led.2019.2923085. [Online]. Available: https://doi.org/10.1109/led.2019.2923085.

[33] A. Krishna, A. Raj, N. Hatui, *et al.*, "AlGaN/GaN Superlattice-Based p-Type Field-Effect Transistor with Tetramethylammonium Hydroxide Treatment," *physica status solidi (a)*, vol. 217, no. 7, p. 1 900 692, Apr. 2020. DOI: 10.1002/pssa.201900692. [Online]. Available: https://doi.org/10.1002/pssa.201900692.

[34] S. Hasenöhrl, P. Chauhan, E. Dobročka, *et al.*, "Generation of hole gas in non-inverted InAl(Ga)N/GaN heterostructures," *Applied Physics Express*, vol. 12, no. 1, p. 014 001, Jan. 2019. DOI: 10.7567/1882-0786/aaef41. [Online]. Available: https://doi.org/10.7567/1882-0786/aaef41.

[35] M. Hiroki, Y. Oda, N. Watanabe, *et al.*, "Unintentional Ga incorporation in metalorganic vapor phase epitaxy of In-containing III-nitride semiconductors," *Journal of Crystal Growth*, vol. 382, pp. 36–40, Nov. 2013. DOI: 10.1016/j.

jcrysgro.2013.07.034. [Online]. Available: https://doi.org/10.1016/j.jcrysgro.2013.07.034.

[36] P. Chauhan, S. Hasenöhrl, Ľ. Vančo, *et al.*, "A systematic study of MOCVD reactor conditions and Ga memory effect on properties of thick InAl(Ga)N layers: A complete depth-resolved investigation," *CrystEngComm*, vol. 22, no. 1, pp. 130–141, Jan. 2020. DOI: 10.1039/c9ce01549c. [Online]. Available: https://doi.org/10.1039/c9ce01549c.

[37] NobelPrize.org. "The Nobel Prize in Physics 2014." (Jan. 2014), [Online]. Available: https://www.nobelprize.org/prizes/physics/2014/summary/.

[38] H. Amano, M. Kito, K. Hiramatsu, and I. Akasaki, "P-Type Conduction in Mg-Doped GaN Treated with Low-Energy Electron Beam Irradiation (LEEBI)," *Japanese Journal of Applied Physics*, vol. 28, no. 12A, p. L2112, Dec. 1989. DOI: 10.1143/jjap.28.l2112.

[39] D. J. Kim, D. Y. Ryu, N. A. Bojarczuk, *et al.*, "Thermal activation energies of Mg in GaN:Mg measured by the Hall effect and admittance spectroscopy," *Journal of Applied Physics*, vol. 88, no. 5, pp. 2564–2569, Sep. 2000. DOI: 10.1063/1.1286925. [Online]. Available: https://doi.org/10.1063/1.1286925.

[40] W. Götz, N. M. Johnson, J. Walker, D. P. Bour, and R. A. Street, "Activation of acceptors in Mg-doped GaN grown by metalorganic chemical vapor deposition," *Applied Physics Letters*, vol. 68, no. 5, pp. 667–669, Jan. 1996. DOI: 10.1063/1.116503. [Online]. Available: https://doi.org/10.1063/1.116503.

[41] S. Brochen, J. Brault, S. Chenot, A. Dussaigne, M. Leroux, and B. Damilano, "Dependence of the Mg-related acceptor ionization energy with the acceptor concentration in p-type GaN layers grown by molecular beam epitaxy," *Applied Physics Letters*, vol. 103, no. 3, p. 032 102, Jul. 2013. DOI: 10.1063/1.4813598. [Online]. Available: https://doi.org/10.1063/1.4813598.

[42] M. Katsuragawa, S. Sota, M. Komori, *et al.*, "Thermal ionization energy of Si and Mg in AlGaN," *Journal of Crystal Growth*, vol. 189-190, pp. 528–531, Jun. 1998. DOI: 10.1016/s0022-0248(98)00345-5.

[43] W. Götz, N. M. Johnson, C. Chen, H. Liu, C. Kuo, and W. Imler, "Activation energies of Si donors in GaN," *Applied Physics Letters*, vol. 68, no. 22, pp. 3144–3146, May 1996. DOI: 10.1063/1.115805. [Online]. Available: https://doi.org/10.1063/1.115805.

[44] A. Castiglia, J.-F. Carlin, and N. Grandjean, "Role of stable and metastable Mg–H complexes in p-type GaN for cw blue laser diodes," *Applied Physics Letters*, vol. 98, no. 21, p. 213 505, May 2011. DOI: 10.1063/1.3593964. [Online]. Available: https://doi.org/10.1063/1.3593964.

[45] S. Nakamura, T. Mukai, M. S. Masayuki Senoh, and N. I. Naruhito Iwasa, "Thermal Annealing Effects on P-Type Mg-Doped GaN Films," *Japanese Journal of Applied Physics*, vol. 31, no. 2B, p. L139, Feb. 1992. DOI: 10.1143/jjap.31.l139. [Online]. Available: https://doi.org/10.1143/jjap.31.l139.

[46] G. Miceli and A. Pasquarello, "Self-compensation due to point defects in Mg-doped GaN," *Physical Review B*, vol. 93, no. 16, Apr. 2016. DOI: 10.1103/physrevb.93.165207. [Online]. Available: https://doi.org/10.1103/physrevb.93.165207.

[47] J. Simon, V. Protasenko, C. Lian, H. Xing, and D. Jena, "Polarization-Induced Hole Doping in Wide–Band-Gap Uniaxial Semiconductor Heterostructures," *Science*, vol. 327, no. 5961, pp. 60–64, Jan. 2010. DOI: 10.1126/science.1183226. [Online]. Available: https://doi.org/10.1126/science.1183226.

[48] P. Kozodoy, Y. P. Smorchkova, M. Hansen, *et al.*, "Polarization-enhanced Mg doping of AlGaN/GaN superlattices," *Applied Physics Letters*, vol. 75, no. 16, pp. 2444–2446, Oct. 1999. DOI: 10.1063/1.125042. [Online]. Available: https://doi.org/10.1063/1.125042.

[49] H. Sakurai, T. Narita, M. Omori, *et al.*, "Redistribution of Mg and H atoms in Mg-implanted GaN through ultra-high-pressure annealing," *Applied Physics Express*, vol. 13, no. 8, p. 086 501, Aug. 2020. DOI: 10.35848/1882-0786/aba64b. [Online]. Available: https://doi.org/10.35848/1882-0786/aba64b.

[50] J. Chen and W. D. Brewer, "Ohmic Contacts on p-GaN," *Advanced Electronic Materials*, vol. 1, no. 8, p. 1 500 113, Aug. 2015. DOI: 10.1002/aelm.201500113. [Online]. Available: https://doi.org/10.1002/aelm.201500113.

[51] G. Greco, F. Iucolano, and F. Roccaforte, "Ohmic contacts to Gallium Nitride materials," *Applied Surface Science*, vol. 383, pp. 324–345, Oct. 2016. DOI: 10.1016/j.apsusc.2016.04.016. [Online]. Available: https://doi.org/10.1016/j.apsusc.2016.04.016.

[52] H. Hahn, B. Reuters, A. Pooth, *et al.*, "P-Channel Enhancement and Depletion Mode GaN-Based HFETs With Quaternary Backbarriers," *IEEE Transactions on Electron Devices*, vol. 60, no. 10, pp. 3005–3011, Oct. 2013. DOI: 10.1109/ted.2013.2272330. [Online]. Available: https://doi.org/10.1109/ted.2013.2272330.

[53] O. Pohorelec, M. Ťapajna, D. Gregušová, *et al.*, "Investigation of interfaces and threshold voltage instabilities in normally-off MOS-gated InGaN/AlGaN/GaN HEMTs," *Applied Surface Science*, vol. 528, p. 146 824, Oct. 2020. DOI: 10.1016/j.apsusc.2020.146824. [Online]. Available: https://doi.org/10.1016/j.apsusc.2020.146824.

[54] W. H. Rippard, A. C. Perrella, F. J. Albert, and R. A. Buhrman, "Ultrathin Aluminum Oxide Tunnel Barriers," *Physical Review Letters*, vol. 88, no. 4, Jan. 2002. DOI: 10.1103/physrevlett.88.046805. [Online]. Available: https://doi.org/10.1103/physrevlett.88.046805.

[55] M. Ťapajna, J. Drobný, F. Gucmann, *et al.*, "Impact of oxide/barrier charge on threshold voltage instabilities in AlGaN/GaN metal-oxide-semiconductor heterostructures," *Materials Science in Semiconductor Processing*, vol. 91, pp. 356–361, Mar. 2019. DOI: 10.1016/j.mssp.2018.12.012. [Online]. Available: https://doi.org/10.1016/j.mssp.2018.12.012.

[56] C. Ostermaier, P. Lagger, M. Reiner, and D. Pogany, "Review of bias-temperature instabilities at the III-N/dielectric interface," *Microelectronics Reliability*, vol. 82, pp. 62–83, Mar. 2018. DOI: 10.1016/j.microrel.2017.12.039. [Online]. Available: https://doi.org/10.1016/j.microrel.2017.12.039.

[57] J. Kuzmík, O. Pohorelec, S. Hasenöhrl, *et al.*, "Mg Doping of N-Polar, In-Rich InAlN," *Materials*, vol. 16, no. 6, p. 2250, Mar. 2023. DOI: 10.3390/ma16062250. [Online]. Available: https://doi.org/10.3390/ma16062250.

[58] J. Kuzmík, A. Adikimenakis, M. Ťapajna, *et al.*, "InN: Breaking the limits of solid-state electronics," *AIP Advances*, vol. 11, no. 12, p. 125 325, Dec. 2021. DOI: 10.1063/5.0066340. [Online]. Available: https://doi.org/10.1063/5.0066340.

[59] M. K. Michihiko Kariya, S. N. Shugo Nitta, S. Y. Shigeo Yamaguchi, H. A. Hiroshi Amano, and I. A. Isamu Akasaki, "Mosaic Structure of Ternary Al $_{1-x}$In$_x$N Films on GaN Grown by Metalorganic Vapor Phase Epitaxy," *Japanese Journal of Applied Physics*, vol. 38, no. 9A, p. L984, Sep. 1999. DOI: 10.1143/jjap.38.l984. [Online]. Available: https://doi.org/10.1143/jjap.38.l984.

[60] S. Hasenöhrl, E. Dobročka, R. Stoklas, F. Gucmann, A. Rosová, and J. Kuzmík, "Growth and Properties of N-Polar InN/InAlN Heterostructures," *physica status solidi (a)*, vol. 217, no. 19, p. 2 000 197, Oct. 2020. DOI: 10.1002/pssa.202000197. [Online]. Available: https://doi.org/10.1002/pssa.202000197.

[61] K. Ko, K. Lee, B. So, *et al.*, "Mg-compensation effect in GaN buffer layer for AlGaN/GaN high-electron-mobility transistors grown on 4H-SiC substrate," *Japanese Journal of Applied Physics*, vol. 56, no. 1, p. 015 502, Jan. 2017. DOI: 10.7567/jjap.56.015502. [Online]. Available: https://doi.org/10.7567/jjap.56.015502.

[62] P. G. Eliseev, "The red $\sigma 2$/kT spectral shift in partially disordered semiconductors," *Journal of Applied Physics*, vol. 93, no. 9, pp. 5404–5415, May 2003. DOI: 10.1063/1.1567055. [Online]. Available: https://doi.org/10.1063/1.1567055.

[63] P. D. C. King, T. D. Veal, A. Adikimenakis, *et al.*, "Surface electronic properties of undoped InAlN alloys," *Applied Physics Letters*, vol. 92, no. 17, p. 172 105, Apr. 2008. DOI: 10.1063/1.2913765. [Online]. Available: https://doi.org/10.1063/1.2913765.

[64] S. Lu, M. Deki, T. Kumabe, *et al.*, "Lateral p-type GaN Schottky barrier diode with annealed Mg ohmic contact layer demonstrating ideal current–voltage characteristic," *Applied Physics Letters*, vol. 122, no. 14, p. 142 106, Apr. 2023. DOI: 10.1063/5.0146080. [Online]. Available: https://doi.org/10.1063/5.0146080.

[65] D. Gregušová, L. Tóth, O. Pohorelec, *et al.*, "InGaN/(GaN)/AlGaN/GaN normally-off metal-oxide-semiconductor high-electron mobility transistors with etched access region," *Japanese Journal of Applied Physics*, vol. 58, no. SC, SCCD21, Jun. 2019. DOI: 10.7567/1347-4065/ab06b8. [Online]. Available: https://doi.org/10.7567/1347-4065/ab06b8.

[66] F. Gucmann, M. Ťapajna, O. Pohorelec, Š. Haščík, K. Hušeková, and J. Kuzmík, "Creation of Two-Dimensional Electron Gas and Role of Surface Donors in III-N Metal-Oxide-Semiconductor High-Electron Mobility Transistors," *physica status solidi (a)*, vol. 215, no. 24, p. 1 800 090, Dec. 2018. DOI: 10.1002/pssa.201800090. [Online]. Available: https://doi.org/10.1002/pssa.201800090.

[67] R. Kúdela, J. Šoltýs, M. Kučera, *et al.*, "Technology and application of in-situ AlOx layers on III-V semiconductors," *Applied Surface Science*, vol. 461, pp. 33–38, Dec. 2018. DOI: 10.1016/j.apsusc.2018.06.229. [Online]. Available: https://doi.org/10.1016/j.apsusc.2018.06.229.

[68] D. Gregušová, E. Dobročka, P. Eliáš, *et al.*, "GaAs Nanomembranes in the High Electron Mobility Transistor Technology," *Materials*, vol. 14, no. 13, p. 3461, Jun. 2021. DOI: 10.3390/ma14133461. [Online]. Available: https://doi.org/10.3390/ma14133461.

[69] F. Gucmann, D. Gregusova, L. Valik, *et al.*, "DC and pulsed IV characterisation of AlGaN/GaN MOS-HEMT structures with Al_2O_3 gate dielectric prepared by various techniques," in *2016 11th International Conference on Advanced Semiconductor Devices & Microsystems (ASDAM)*, IEEE, Nov. 2016. DOI: 10.1109/asdam.2016.7805883. [Online]. Available: https://doi.org/10.1109/asdam.2016.7805883.

[70] M. Tapajna, K. Husekova, O. Pohorelec, *et al.*, "Effect of HCl pretreatment on the oxide/semiconductor interface state density in AlGaN/GaN MOS-HEMT structures with MOCVD grown $A1_2O_3$ gate dielectric," in *2016 11th International Conference on Advanced Semiconductor Devices & Microsystems (ASDAM)*, IEEE, Nov. 2016. DOI: 10.1109/asdam.2016.7805931. [Online]. Available: https://doi.org/10.1109/asdam.2016.7805931.

[71] D. Gregušová, M. Blaho, O. Pohorelec, *et al.*, "GaAs nanomembranes in device technology," in *SURFINT - SREN IV 2019*, Slovakia: Comenius University Bratislava, Jan. 2019, pp. 136–137, ISBN: 978-80-223-4811-9.

[72] D. Gregušová, O. Pohorelec, M. Ťapajna, *et al.*, "Polarization engineering in GaN-based devices," in *2021 International Meeting for Future of Electron Devices*, Kansai: IEEE, Jan. 2021, pp. 1–4, ISBN: 978-1-6654-4200-8.

[73] O. Pohorelec, M. Ťapajna, D. Gregušová, *et al.*, "Investigation of interfaces and threshold voltage instabilities in MOS-gated InGaN/AlGaN/GaN HEMTs," in *SURFINT – SREN IV 2019*, Slovakia: Comenius University Bratislava, Jan. 2019, pp. 136–137, ISBN: 978-80-223-4811-9.

[74] O. Pohorelec, S. Hasenöhrl, M. Blaho, *et al.*, "Mg doping in In-rich InAlN layers," in *2022 International Workshop on Nitride Semiconductors*, Germany: IWN2022, Jan. 2022, p. 255.

[75] O. Pohorelec, M. Ťapajna, D. Gregušová, K. Frohlich, and J. Kuzmík, "Investigation of threshold voltage instabilities in MOS-gated InGaN/AlGaN/GaN HEMTs," in *ADEPT 2019 : 7th International Conference on Advances in Electronic and Photonic Technologies*, Slovakia: University of Žilina, Jan. 2019, pp. 123–126, ISBN: 978-80-554-1568-0.

[76] M. Ťapajna, F. Egyenes, S. Hasenöhrl, *et al.*, "Investigation of GaN P-N junction processed by Mg ion implantation," in *ADEPT 2019 : 7th International Conference on Advances in Electronic and Photonic Technologies*, Slovakia: University of Žilina, Jan. 2019, ISBN: 978-80-554-1568-0.

[77] O. Pohorelec, D. Gregušová, S. Hasenöhrl, *et al.*, "Mg doping of InAlN layers," in *ADEPT 2021 : 9th International Conference on Advances in Electronic and Photonic Technologies*, Slovakia: Univ. Zilina in EDIS-Publishing Centre of UZ, Jan. 2021, pp. 147–150, ISBN: 978-80-554-1806-3.